Crustacean Research 2022 Vol.51: 55–89

 doi: 10.18353/crustacea.51.0_55

The Petalophthalmidae (Crustacea: Mysida) of the ANDEEP I–III expeditions to the Antarctic deep sea, with description of a new species and first record of photophores in mysids

Karl J. Wittmann

Abstract.— Three ANDEEP expeditions yielded five Petalophthalmidae species of the genus *Hansenomysis* in 1030–3683 m depth on the floor of the Southern Ocean. *Hansenomysis pseudophthalma* sp. nov. is distinguished by features of the carapace, antenna, and telson. A fully adult specimen is first described for *H. chini*. A world key to the species of *Hansenomysis* is given. Unlike certain previous interpretations, the dactylus of thoracic endopods 3–5 has a single claw opposing a pair of modified paradactylary setae. Propodus and dactylus 6–8 are separate, not fused, and bear a smooth nail in all *Hansenomysis* species examined. Juveniles were available in three species and start with two bulb-shaped eye rudiments inside a common cuticular sheath forming a transverse bar. The bulbs then flatten, although a bulb-like formation persists until the adult stage; no eyeplate is formed. The carapace bears hepatic bulges resembling eyes in adult *H. pseudophthalma* and *H. chini*. The distal hyaline coat of bulges possibly represents lenses in *H. pseudophthalma* and *H. sorbei*. The modification of bulges is indicative of photophores, described for the first time here in the family Petalophthalmidae. The exclusive occurrence of mature photophores in adults points to possible role in reproductive behavior.

http://zoobank.org/urn:lsid:zoobank.org:pub:8530B295-CF00-413D-830C-C41C685FA467

Key words: Southern Ocean, taxonomy, distribution, post-larval development, luminescent organs

■ Introduction

The ANDEEP (ANtarctic benthic DEEP-sea biodiversity) collections obtained from Polarstern cruises conducted by the University of Hamburg and the Senckenberg Institute (Frankfurt) in 2002 (ANDEEP I, II) and 2005 (ANDEEP III) yielded 59 specimens from five species of the family Petalophthalmidae Czerniavsky, 1882. Species of this family are mainly meso- to bathypelagic and bathybenthic, mostly below 500 m depth. Petryashov (2014) listed five species of *Hansenomysis* Stebbing, 1893, from the Antarctic realm ($>=60°S$) plus *Ceratomysis ericula* Ledoyer, 1977, from subantarctic waters. An own global census from 5 April 2022 highlights 44 species of Petalophthalmidae, contributing 4% to the inventory of 1208 recent species of Mysida Boas, 1883. The preference of most species for cold and deep waters is reflected by a higher percentage of 15%, namely six species of Petalophthalmidae including the below-described new one, contributing to a total of 41 species of Mysida in Antarctic waters. The present publication on Petalophthalmidae contributes to the aims (Brandt *et al.* 2003) of the ANDEEP expeditions by describing a new species

Received: 1 May 2022. Accepted: 9 Jun 2022. Published online: 23 July 2022.

of *Hansenomysis* and by reporting important morphological novelties regarding photophores, post-larval development of reduced eyes, and the structure of thoracic endopods. This contributes to consolidating and broadening our current knowledge on the biodiversity in polar deep waters.

■ Materials and Methods

Materials obtained from the Zoological Museum Hamburg (Germany) were used for elaboration of the collection stock yielded by ANDEEP I–III expeditions of the research vessel Polarstern. Maps and itineraries of ANDEEP cruises are given in Fütterer *et al.* (2003) and Fahrbach (2006). Station and sampling data are available from Fütterer *et al.* (2003), Howe (2003, 2006), Fahrbach (2006), and Brandt *et al.* (2007). A total of 59 specimens of Petalophthalmidae, all belonging to the genus *Hansenomysis*, were obtained by ANDEEP I in Jan.–Feb. 2002 in the Drake Passage and the South Shetland area, by ANDEEP II in Mar. 2002 in the Weddell Sea, and by ANDEEP III in Feb.–Mar. 2005 in the Weddell Sea and the Powell Basin. The respective materials were obtained from a depth range of 1030–3683 m with self-closing epibenthic sledges equipped with epinet and supranet, each with mesh-size 0.3 mm, as detailed by Brandt *et al.* (2006).

Materials including the here defined types were returned to the Zoological Museum of Hamburg in vials with aqueous solution of ethanol 80% with propylene glycol 10% unless explicitly stated as having been dissected and mounted on slides. Terminology, measurements, preparation, microscopy, and documentation as in Wittmann & Chevaldonné (2021). By convention the lateral portions of the carapace in front of the cervical sulcus are termed 'hepatic region' and the teeth therein 'hepatic teeth', although some hepatic caeca are found more dorsally outside this area. Bulges in this area are here termed 'hepatic bulges' some of which bear 'hepatic teeth'. As shown below, the here studied eye rudiments are united in a transverse bar with distolateral processes rather than a plate, therefore termed 'eye rudiments' rather than using the traditional term 'eye-plates'. 'Apex' is used for structures with acute or narrowly blunt end, 'terminus' for broader ends. Unlike 'nails' the 'claws' are hook-like; the term 'nail' also used to indicate the absence of such elements. Without any additional morphological implications 'tarsus' is used for segments distal to the 'knee', and 'carpopropodus' for the single segment between the 'knee' and the distal, mostly claw-bearing dactylus. Diagnoses of genus and species are designed for distinction of all the respective known taxa. Some heterogeneity of the diagnoses reflects currently unknown data on the adults of both sexes.

Abbreviations

BL = body length measured from tip of rostrum to terminal margin of telson
ZMH = Zoological Museum Hamburg
#I = station numbers of expedition ANDEEP I
#II = station numbers of expedition ANDEEP II
#III = station numbers of expedition ANDEEP III

■ Taxonomic Account

Family Petalophthalmidae Czerniavsky, 1882
Subfamily Hansenomysinae Wittmann, Ariani & Lagardère, 2014
Genus ***Hansenomysis*** Stebbing, 1893

Selected References:

Arctomysis Hansen, 1887: 210 (new taxon); Stebbing, 1893: 267 (concluded as junior homonym of *Arctomysis* Czerniavsky, 1887).

Hansenomysis Stebbing, 1893: 267 (replacement name); Birstein & Tchindonova, 1970: 277–

280 (description, synonymy); Petryashov, 2005: 962, 969 (distribution, biogeography, in key); San Vicente, 2010: 36, 59 (diagnosis, in key to Antarctic taxa); Wittmann, 2020: 30–31 (mouthpart morphology, feeding type); Astthorsson & Brattegard, 2022: 20–24 (species records off Iceland); Mees & Meland, 2022: AphiaID 119913 (accepted).

Diagnosis.—Hansenomysinae with eyes fused to single, small, transversely implanted rudiment without visual elements. Rudiment with rostrally projecting processes. Basal segment of antennula dorsally with Tattersall organ. Antennula with strong sexual dimorphism, trunk and lateral flagellum modified and thickened in males, normal in females. Antennal scale unsegmented, inner margin with setae, outer margin with setae and spines. Thoracopod 1 without exopod, thoracopods 2–8 with well-developed exopod. Carpopropodus of thoracic endopods 3–5 unsegmented, apex with dense brush of setae surrounding small dactylus with small claw (opposing two modified paradactylary setae in most or all ? species); endopods 6–8 with unhidden dactylus longer than wide, nail comparatively long and slender. Female pleopods reduced to setose rods. Male pleopods biramous, endopod 1 unsegmented, endopods 2–4 and all exopods multisegmented. Endopod of uropods unsegmented, setose all around; exopod 2-segmented by means of subterminal suture, distal segment setose all around, basal segment with setose mesial margin and species-specifically furnished lateral margin. Telson mid-terminally convex or at most weakly concave, not incised; its margins with spines, no setae.

Type species.—*Arctomysis Fyllae* Hansen, 1887, by original designation. Taxon currently accepted as *Hansenomysis fyllae* (Hansen, 1887).

Species inventory and distribution.—Nineteen species including the new one. Data on distribution modified and updated from Bravo & Murano (1997), Brandt *et al.* (1998), Price (2001, 2004), Fukuoka (2009), San Vicente (2010), and Astthorsson & Brattegard (2022).

H. anaramosae San Vicente & Sorbe, 2008, Bellingshausen Sea, Weddell Sea, 65–71°S, 540–2086 m depth.

H. angusticauda O. S. Tattersall, 1961, Ross Sea, Palmer Archipelago, NE of Elephant Island, Antarctic Peninsula, Weddell Sea, 61°S–75°S, 160–2893 m.

H. antarctica Holt & Tattersall, 1906, circum-Antarctic, 53°S–76°S, 100–400 m.

H. armata Birstein & Tchindonova, 1958, Kurile-Kamchatka Trench, off Japan, 35° N–50°N, 2960–3308 m.

H. carinata Casanova, 1993, New Caledonia, 23°S, 950–1000 m.

H. chini Băcescu, 1971, Peru Trench, Weddell Sea, 08°S–71°S, 1119–3103 m.

H. falklandica O. S. Tattersall, 1955, Falkland Islands (Malvinas), Patagonia, Magellan Strait, off Iceland, 63°N–53°S, 175–1919 m.

H. fyllae (Hansen, 1887), North Atlantic (off Greenland, Iceland, Ireland, US east coast), 40°N–70°N, 150–1778 m.

H. japonica Bravo & Murano, 1997, off Japan, 35°N, 590 m.

H. lucifugus (Faxon, 1893), off Galapagos, 00°, 2418 m (? Japan, 35°N, 742 m).

H. menziesi Băcescu, 1971, Peru Trench, 08°S, 1927–1997 m.

H. nouveli Lagardère, 1983, Bay of Biscay, Rockall Trough, off Iceland, 44°N–64°N, 1121–2498 m.

H. pseudophthalma sp. nov., Weddell Sea, Powell Basin, N of South Shetland Islands, 62°S–71°S, 2659–3103 m.

H. pseudofyllae Lagardère, 1983, Bay of Biscay, 44°N–48°N, 1950–4829 m.

H. rostrata Birstein & Tchindonova, 1970, Kurile-Kamchatka Trench, off Japan, 40°N–44°N, 4690–4951 m.

H. sorbei San Vicente, 2009, Bellingshausen Sea, Powell Basin, 63°S–70°S, 1579–1869 m.

H. spenceri Băcescu, 1971, Peru Trench, 08°S, 1927–1997 m.
*H. tropicali*s Băcescu, 1967, Peru Trench, 08°S, 1927–1997 m.
H. violacea (Birstein & Tchindonova, 1958), Kurile-Kamchatka Trench, 44°N, 1050–1070 m.

World key to the species of *Hansenomysis*

Modified and updated from Bravo & Murano (1997).

1 Carapace without tooth-like processes, not counting processes from anterior margin 9
– Carapace with acute or blunt, tooth-like processes 2
2 Posterior margin of pleomere 3 without tooth-like processes 4
– Posterior margin of pleomere 3 with tooth-like processes 3
3 Carapace with small triangular rostrum ..... *H. menziesi* Băcescu, 1971
– Carapace anteriorly rounded, without rostrum ..... *H. sorbei* San Vicente, 2009
4 Lateral margin of antennal scale without setae between spines 7
– Lateral margin of antennal scale with setae at least between distalmost spines 5
5 Carapace with teeth in the gastric and hepatic regions 6
– Carapace without teeth in the gastric and hepatic regions ..... *H. falklandica* O. S. Tattersall, 1955
6 Midline of carapace with a single strong tooth shortly behind cervical sulcus (not counting teeth elsewhere) ..... *H. armata* Birstein & Tchindonova, 1958
– Midline of carapace with cluster of four densely set humps or teeth shortly behind cervical sulcus ..... *H. pseudophthalma* sp. nov.
7 Carapace anteriorly produced into a small acute rostrum ..... *H. anaramosae* San Vicente & Sorbe, 2008
– Anterior margin of carapace evenly rounded in median portions, no rostrum 8
8 Telson length three times maximum width ..... *H. antarctica* Holt & Tattersall, 1906
– Telson length 4–5 times maximum width ..... *H. angusticauda* O. S. Tattersall, 1961
9 Eye rudiment with an unpaired median process; carapace mid-anteriorly well rounded, without rostrum ..... *H. nouveli* Lagardère, 1983
– Eye rudiment with paired processes only 10
10 Eye rudiment with spoon-like anterior processes ..... *H. carinata* Casanova, 1993
– Eye rudiment with lateral or paramedian anterior processes other than spoon-like 11
11 Lateral margin of antennal scale with at least one spine on distal half 16
– Lateral margin of antennal scale without spines on distal half 12
12 Carapace anteriorly produced into acute rostrum 13
– Anterior margin of carapace evenly rounded in median portions, without rostrum 14
13 Antennal scale extends by more than one-third its length beyond antennular trunk ..... *H. rostrata* Birstein & Tchindonova, 1970
– Antennal scale extends by less than one-third its length beyond antennular trunk ..... *H. lucifugus* (Faxon, 1893)
14 Antennal scale shorter than antennal peduncle, lateral margin of antennal scale with one spine ..... *H. tropicali*s Băcescu, 1967
– Antennal scale longer than antennal peduncle, lateral margin of antennal scale with more than two spines 15
15 Telson length four times maximum width; proximal 2/3 with about parallel lateral margins

H. japonica Bravo & Murano, 1997

– Telson length 5/2 maximum width; proximal 4/5 with straight, diverging lateral margins ..... *H. violacea* (Birstein & Tchindonova, 1958)

16 Lateral margin of antennal scale with spines only on distal half, telson without spines on proximal half ..... *H. pseudofyllae* Lagardère, 1983

– Lateral margin of antennal scale with spines on (part of) proximal as well as distal half 17

17 Antennal peduncle extends beyond antennal scale 18

– Antennal peduncle shorter than antennal scale; telson without spines on basal half ..... *H. fyllae* (Hansen, 1887)

18 Distal spine not reaching to tip of antennal scale; antennal scale extends shortly beyond antennular trunk ..... *H. spenceri* Băcescu, 1971

– Distal spine extends beyond tip of antennal scale; antennal scale not extending beyond antennular trunk ..... *H. chini* Băcescu, 1971

Hansenomysis chini Băcescu, 1971
Figs. 1, 10C, 11A, F, P, K

Selected references:

Hansenomysis chini Băcescu, 1971: 9–10, Figs. 8–9 (first description); Mauchline & Murano, 1977: 57 (in catalogue); Bravo & Murano, 1997: 234 (in key); Price, 2004: 56 (in list); Mees & Meland, 2022: AphiaID 226371 (accepted).

Material examined.—Weddell Sea: 2 ♀♀ imm., BL 10.3–12.0 mm, 2 juv. 5.5–7.1 mm, #II-132-2, 65.2957°S 53.3803°W to 65.2927°S 53.3805°W, 2086 m, 6 Mar. 2002, epinet; 1 ♀ subad. 11.9 mm, 1 imm. 9.1 mm, same haul as before, supranet; 1 juv. 6.3 mm, #II-133-3, 65.3358°S 54.2392°W to 65.3343°S 54.2418° W, 1122–1119 m, 7 Mar. 2002, epinet; 1 ♀ ad. 16.3 mm, damaged, brood pouch empty, ovarian tubes filled with large eggs, on slides, #III-080-9, 70.6512°S 14.7227°W to 70.6537°S 14.7232°W, 3103–3102 m, 23 Feb. 2005, supranet.

Diagnosis.—Based on females only. All female features of generic diagnosis. Eye rudiment shortly projecting beyond anterior margin of carapace; rudiment with pair of small lateral, anteriorly directed, distally rounded, sub-triangular processes (Fig. 10C), no additional processes. Antennal scale 4–5 times as long as wide, reaching almost to terminus of antennular trunk. Scale ends by 8–26% its length proximally from terminus of antennal peduncle. Proximal 2/5 of antennal scale with smooth outer margin, median 2/5 with 6–7 spines distally increasing in size, no setae between spines. Distal fifth of antennal scale forms a setose lobe without spines. Distalmost spine extends beyond this lobe. Carapace with anterior margin broadly rounded and slightly up-tilted; apart from this no distinct rostrum; anterior margin with pair of disto-sublateral triangular projections (Fig. 10C). Carapace on each side with hepatic bulge in front of large fold which runs obliquely mesially (Fig. 1A) and then turns caudally until meeting its bilateral counterpart in a 'U'-shaped manner at the midline about one-sixth carapace length in front of posterior margin of carapace. Short median crest starts with acute upper edge at fold's meeting point and continues along midline up to shortly in front of posterior margin. No teeth on carapace, no spines, no setae. Thoracomeres 6–8 with dorsally up-tilted anterior margin, most strongly in thoracomere 7. Thoracomeres 6–8 and pleomeres 1–3 without spines or teeth. Posterior margin of pleon-pleurites 4, 5 on each side produced with small caudal tooth-like protrusion above ventro-lateral edge. Posterior margin of pleomere 6 with ventro-lateral

edges produced into a small tooth and with a larger, tooth-like triangular protrusion formed by the scutellum paracaudale. Female pleopods 1–4 unsegmented; pleopod 5 long, 2-segmented, extending beyond pleomere 6. Outer margin of proximal segment of exopod of uropods with 6–8 spines increasing in length distally. Distalmost spine extends beyond the setose apical segment. Telson linguiform, 3–4 times as long as wide, proximal 65–75% with (al-

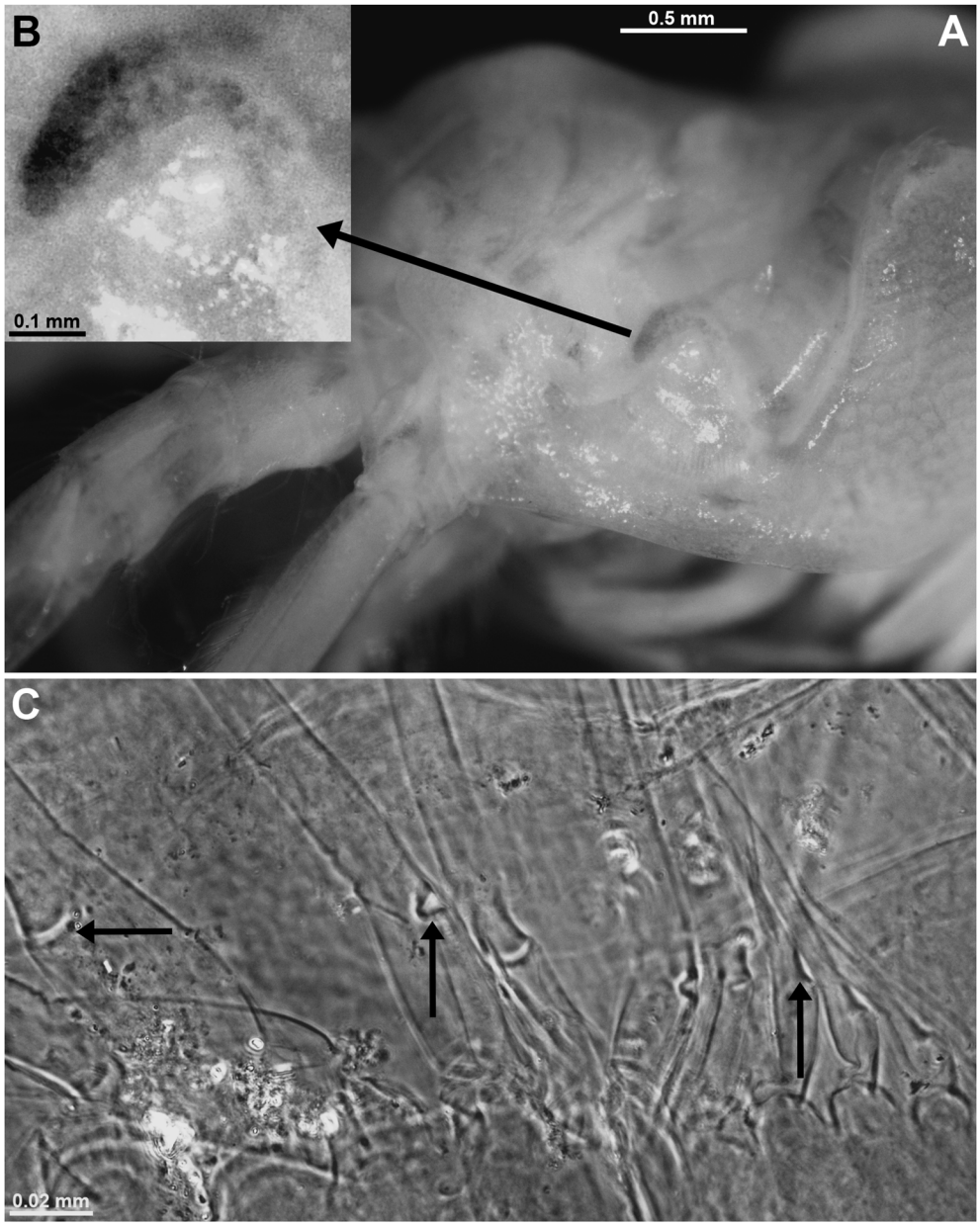

Fig. 1. *Hansenomysis chini* Băcescu, 1971, adult female with BL 16.3 mm. A, cephalic region, lateral; B, detail of panel (A) showing hepatic bulge; C, series of modified setae on basal segment of left antennular trunk, note size of setae increasing laterally (from right to left), arrows point to diverse indentations near setae basis.

most) parallel lateral margins, distal 25–35% converging to a broadly rounded convex terminus. Proximal 20–30% with smooth margins, distally subsequent 15% with small spines continuously increasing in length distally; remaining distal portions of lateral margin with series of large spines with small spines in between. Penultimate large spine about one-fifth telson length and by far the overall longest. It reaches to about terminus of telson. Convex terminal margin of telson with two pairs of large lateral spines flanking a small median spine. Telson extends beyond both rami of uropods.

Descriptive notes.—The non-adults correspond very well with the description of a single subadult female by Băcescu (1971). Small meristic differences probably reflect differences in size and development as well as individual variation: in the present samples the only subadult and the largest among three immature females are 11.9 and 12.0 mm long, respectively, measured from the anterior margin of the carapace to the terminal margin of the telson. This fits with the size of the holotype, a 12-mm-long non-adult female measured by Băcescu (1971) from the tip of the antennular peduncle to the extrapolated (broken) end of the telson. Present antennal scale with seven spines in the subadult and 6–7 in immatures; exopod of uropods with six spines in the subadult and 4–7 in immatures. The five apical spines of the telson slightly hispid along their proximal portions. The present (damaged) adult female is the first adult specimen recorded. The sublateral, anterior protrusions of the eye rudiment (Fig. 10C) longer than in non-adults, particularly longer than in the holotype (Băcescu 1971: Fig. 8B). This does not contradict determination at the species level because such protrusions become longer during individual development as also in other here treated species (f.i. Fig. 10D–G). Antennal scale, uropods, and telson damaged in the present adult female; carapace well preserved. Antennular trunk with transverse series of modified setae (Fig. 1C) shortly behind distal margin of basal segment (as in *H. pseudophthalma* sp. nov.: Fig. 5B, D, E). Setae modified by indentation near basis (Fig. 1C); size of setae increasing with lateral position. Oostegites 1–7 (from thoracopods 2–8) of the dissected adult female with 0, 1, 2, 2–3, 3, 2, and 1 spine-like seta, respectively; these setae *in loco* invariantly projecting perpendicularly away from outer face. Position and structure of setae as in Fig. 7H, I; setae closely spaced in oostegites 3–6. For eye development, structure of carapace and of thoracic endopods see chapter 'Morphological Account' below.

Occurrence.—Type locality is Peru-Chile Trench, 08.22°S 81.15°W, depth 1927–1997 m (Băcescu, 1971). The present records from the NW-Weddell Sea, 65°S 53–54°W, depth 1119–2086 m, and from Eastern Weddell Slope, 71°S 15°W, depth 3102 m, are the second to fourth ever reported and represent a very strong extension of the known range from the equatorial E-Pacific to the Southern Ocean. The new samples were taken with the epinet as well as supranet of the epibenthic sledge.

Hansenomysis pseudophthalma sp. nov.
http://zoobank.org/urn:lsid:zoobank.org:act:F38E2DA5-C81F-4AB6-81B7-BDCD1FD6B0E9

Figs. 2–8, 11B, G, L, Q

Material examined.—Holotype, ♀ ad. (ZMH 61758), BL 22.8 mm, marsupium empty (Figs. 2A–C, 3A, B, 4F, G), Weddell Sea, #III-080-9, 70.6512°S 14.7227°W to 70.6537°S 14.7232°W, 3103–3102 m, 23 Feb. 2005, supranet.

Paratypes: Weddell Sea: 1 ♂ ad., BL 22.3 mm, 1 ♂ subad. 18.2 mm, 1 juv. 9.9 mm (ZMH 61756), same haul as for holotype, epinet; 2 imm. 11.8–14.0 mm (ZMH 61757), same sampling data as for holotype; 1 ♀ ad. 21.7 mm on slides (ZMH 61752), 1 ♀ subad. 20.4 mm, 1 imm. 10.3 mm, 1 juv. 8.8 mm in

vial (ZMH 61753), #II-131-3, 65.3305°S 51.5270°W to 65.3325°S 51.5235°W, 3049–3050 m, 5 Mar. 2002, epinet; 1 ♂ ad. 22.7 mm on slides (ZMH 61755), 1 ♂ subad. 21.2 mm, 4 imm. 12.7–16.3 mm, 10 juv. 6.9–11.9 mm (ZMH 61754) in separate vial, same sample as before; Powell Basin: 1 imm. 12.7 mm, 1 juv. 5.3 mm (ZMH 61759), entrance to basin at Weddell continental slope, #III-121-11, 63.6288°S 50.6348°W to 63.6258°S 50.6395° W, 2663–2659 m, 15 Mar. 2005, supranet; Drake Passage: 1 ♂ ad. 19.9 mm (ZMH 61751), #I-114-4, 61.7257°S 60.7033°W to 61.7257°S 60.7425°W, 2914–2920 m, 18 Feb. 2002, supranet.

Non-types: Weddell Sea: 1 juv., BL 6.5 mm, #II-131-3, 65.3305°S 51.5270°W to 65.3325°S 51.5235°W, 3049–3050 m, 5 Mar. 2002, epinet; Drake Passage: 1 juv., 5.9 mm, #I-042-2, 59.6715°S 57.5905°W to 59.6737°S 57.5878° W, 3683–3680 m, 27 Jan. 2002, epinet.

Type locality.—Type locality is Eastern Weddell Slope, Kapp Norvegia, SW of Wegener Canyon, sample taken with supranet of epibenthic sledge, start position in 3103 m depth at 70.6512°S 14.7227°W, end position in 3102 m at 70.6537°S 14.7232°W. An additional positive sample was taken there with epinet. The species was also recorded in the NW-Weddell Sea, at the entrance to Powell Basin, and in the S-Drake Passage. Total latitudinal range 60–71°S, depth range 2659–3680 m.

Derivatio nominis.—The species name is a Latinized adjective with feminine ending, formed by linking the Greek adjective *ψευδής* (false) with the noun *ὀφθαλμὸς* (eye), related to the eyelike appearance of the hepatic bulge. Etymological precedence found in the buprestid genus *Pseudophthalma* Thomson, l878, listed as junior synonym of *Polybothris* Spinola, 1837, by Bellamy (2006).

Diagnosis.—Based on adults of both sexes. All features of the generic diagnosis. Transverse eye rudiment with pair of small distolateral processes (Figs. 4C, 5A), no additional processes. Carapace (Fig. 5A) with median portions of anterior margin broadly rounded and slightly up-tilted; apart from this no distinct rostrum. Anterior margin sublaterally with pair of narrowly blunt (almost acute) triangular projections; distolateral edges well rounded. Cephalic region with one large hepatic bulge on each side (Figs. 3A, B, E, 4B). Carapace with series of ridges, small humps and teeth along midline (Figs. 2C, E, 5A): in the gastric region (above foregut) with carina bearing minute to medium-sized denticles along dorsal (outer) circumference; caudally followed by 2–3 small humps each bearing 1–2 small teeth, and behind cervical sulcus a cluster of four densely set small humps or teeth (arrow in Fig. 2E), then 4–5 loosely arranged small teeth, and finally a long, broad longitudinal crest (elevation) reaching almost to posterior margin of carapace. Starting at the cervical sulcus, two sublateral keels run caudally and unite in a 'U'-shaped manner at about one-seventh carapace length from mid-posterior margin. Mesial margin of keels armed with several small teeth. Antennal scale (Figs. 4A, B, 5F, G) length 3–4 times maximum width. In parallel orientation, scale reaching 0–0.1 times its length beyond antennal peduncle; 0.5–0.6 times beyond antennular trunk in males, and 0.3–0.4 beyond longer antennular trunk in females. Proximal sixth of antennal scale with smooth outer margin. This margin with 5–7 spines along the stretch from 1/6 to 2/3 scale length from basis; spines increasing in size distally; the three proximal spines equidistant, without setae in between; the 2–4 distal spines with larger, setose interspaces. Structure of thoracic endopods 3–8 (Figs. 7H–L, 11B, G, L, Q) as given below for five *Hansenomysis* species. Thoracomeres 7, 8 with dorsally up-tilted anterior margin. Posterior margin of pleomeres 4, 5 (Fig. 4F, G) on each side produced with two caudal tooth-like protrusions shortly above ventro-lateral edge in adults (not so in earlier

stages). No additional teeth on pleomeres 1–5. Posterior margin of pleomere 6 with ventro-lateral edges produced into a tooth. The scutellum paracaudale forms an additional, larger, triangular protrusion on posterior margin of pleomere 6. Female pleopod 1 unsegmented, pleopods 2–4 with two segments, pleopod 5 with three segments (Fig. 8A–C). Male pleopods biramous; endopod 1 unsegmented; endopods 2–4 and all exopods multisegmented; endopod 5 rod-like, 3-segmented (Fig. 8D, F, H, I). Basal segment of exopod of uropods (Fig. 8J) with proximally smooth lateral margin; distal 40–50% of lateral margin with dense series of 16–23 spines discontinuously increasing in size caudally; the large distalmost spine clearly shorter than the setose terminal segment. No setae on lateral margin of the basal segment except for one small seta at the edge with the terminal segment. Telson (Figs. 4D, 8L) slender, elongate linguiform in dorsal view, lateral margins about parallel in central portions, terminus convex, well rounded. Length of telson *in loco* (Fig. 4D) four times maximum width (width overestimated in Fig. 8L due to expansion on slide). Telson shortly extending beyond uropods. Proximal fifth of each lateral margin smooth; distal 4/5 of each margin with 35–51 spines, most of which arranged in groups of large spines with small spines in between; distalmost large lateral spines overreaching the terminal margin; terminus in addition with two large spines flanking a shorter median spine; telson of adults with total of 74–104 spines.

Description.—All features of the above diagnosis. Adult females with BL 21.7–22.8 mm (n = 2), adult males with 19.9–22.3 mm (n = 3). Body slender, cephalothorax contributes 32–38% total length, pleon 39–41%, telson 21–27% (Fig. 2A, B). Carapace 22–26% body length. Thorax without mid-sternal processes in both sexes (Fig. 7E). First thoracic sternite with the usual mid-rostral lobe contributing to the caudal closure of the mouth area; lobe in this case hairy (Fig. 7E). No setae or scales found on thoracic sternites 2–8 in both sexes.

Carapace (Figs. 3, 5A): up-tilted stretch in the middle of anterior margin of carapace is 2–3% carapace length. Cervical and cardial sulci well developed. Carapace leaving ultimate three thoracic somites mid-dorsally exposed. Indentation of posterior margin unapparent upon inspection *in loco*, but well visible in carapace detached and expanded on slide (Fig. 5A). For hepatic bulges see chapter 'Morphological Account' below.

Eyes (Figs. 4C, 5A): eye rudiment formed by short transverse bar with caudal half covered by the carapace. Post-larval development of the eye rudiment as described below for four species, though less striking compared with that of *H. anaramosae* (Fig. 10A, B, D–G).

Antennula (Figs. 2B, D, 4A, B, 5B–E): antennular trunk short, only 30–38% carapace length in males, 42–44% in females. In dorsal view, segments 1–3 contribute 44–52%, 19–26%, and 24–30% to total trunk length in males, 37–45%, 32–39%, and 22–28% in females, respectively. Widths are 45–48%, 53–56%, and 50–53% trunk length in males, 32–36%, 28–32%, and 25–29% in females, respectively. Tattersall organ well developed. Basal segment of trunk very similar in both sexes (Fig. 5B, E): small mesial, blunt protuberance at 45% segment length from basis; transverse fan formed by 12–14 smooth setae of varying size placed mesially behind rostral margin on dorsal face. Another transverse series of 6–8 modified setae positioned laterally behind rostral margin on dorsal face. Stout basis of the latter setae with small indentation (Fig. 5D), their flagellum barbed along its subbasal to apical portions. Distal third of basal segment in addition with un-indented, barbed setae. Median and terminal segment of trunk with dense series of plumose setae along mesial margin in females (Fig. 5E). Males with shorter plumose setae, fewer and not in dense series (Fig. 5B). Small semicircular lobe mid-dorsally extending shortly beyond anterior

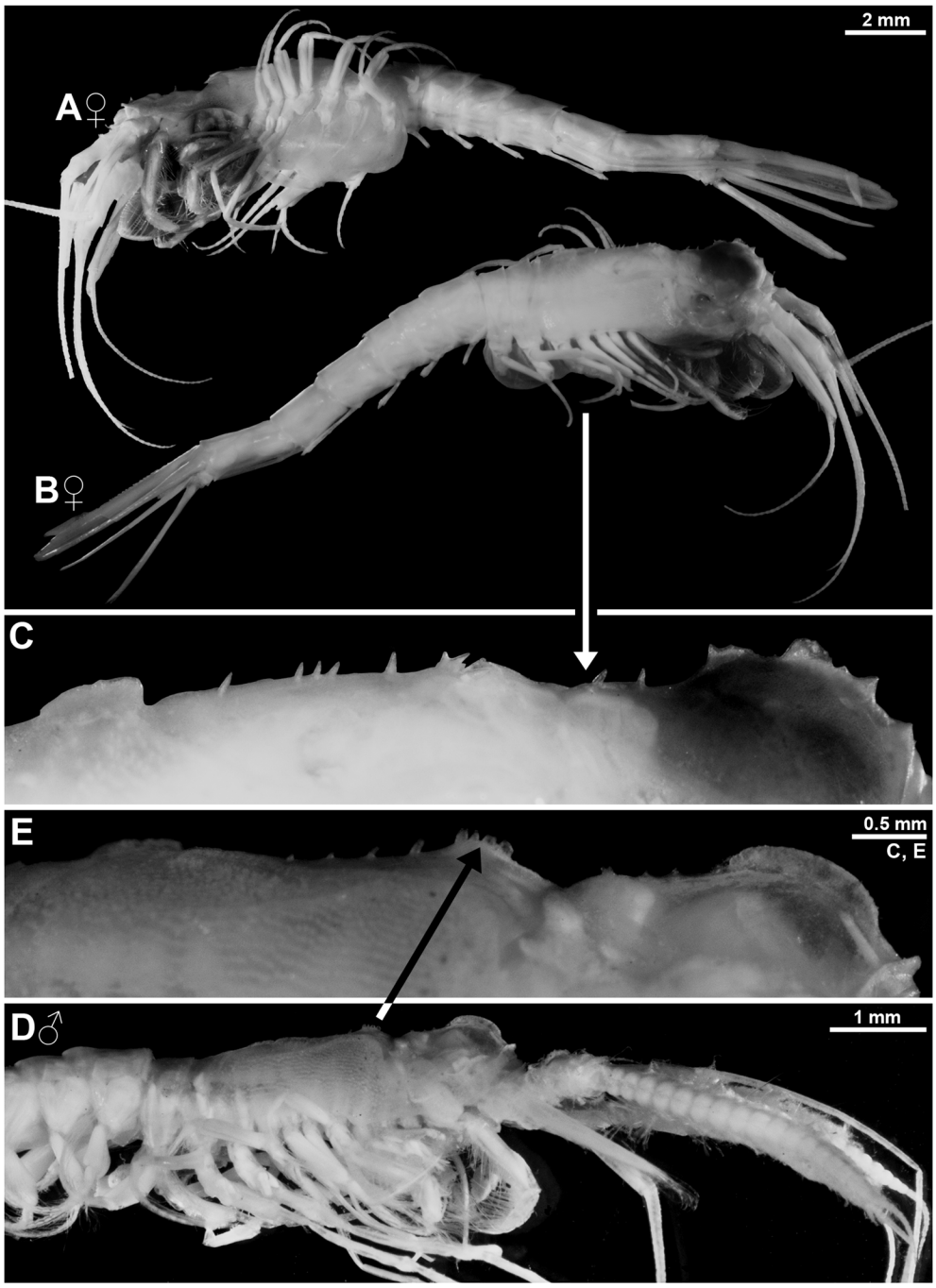

Fig. 2. *Hansenomysis pseudophthalma* sp. nov., holotype, adult female with BL 22.8 mm (A–C) and paratype, adult male 22.7 mm (D, E). A, B, holotype *in toto*, obliquely ventral (A) and lateral (B); C, detail of panel (B) showing armature of carapace along dorsal midline; D, anterior half of male paratype, lateral; E, detail of panel (D) showing armature of carapace along dorsal midline, arrow starts (D) and ends (E) at cluster of four blunt teeth. A–C, objects artificially separated from background.

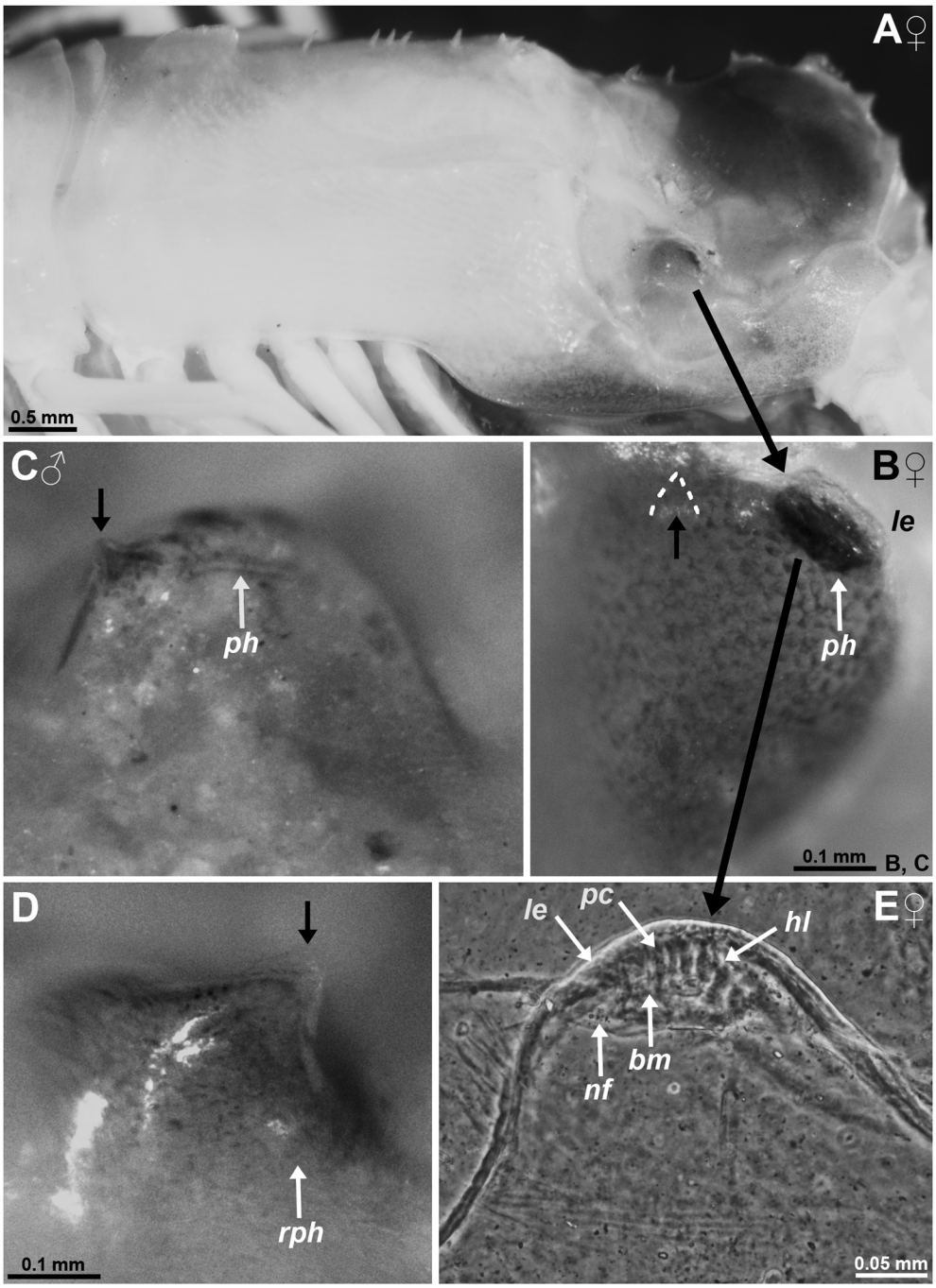

Fig. 3. Hepatic bulges in *Hansenomysis pseudophthalma* sp. nov., holotype, adult female with BL 22.8 mm (A, B), paratypes, adult male 22.3 mm (C), immature 11.8 mm (D), and adult female 21.7 mm (E). A, cephalothorax, lateral, detail (B) shows hepatic bulge; B–D, hepatic bulges in series of decreasing body size, right (B, D) and left (C) bulges in lateral view, small black arrows in panels B–D point to (sub)-apical spines, dashed line in panel B enhances contrast of small tooth; E, hepatic bulge with photophore dissected and expanded on slide (in other adult female than in panel B). Labels indicate basement membrane (*bm*), haemolymph lacunary system (*hl*), lens (*le*), nerve fibers (*nf*), photocytes (*pc*), photophore (*ph*), and rudiment of photophore (*rph*).

margin of terminal segment in both sexes. Circumference of lobe distolaterally with 3–4 apically barbed setae and disto-mesially with series of minute barbs, no spines, no teeth. Antennular flagella (Fig. 5B, E) long, multisegmented, setose in adults of both sexes. Both female flagella about equally wide near basis (Fig. 5E); mesial flagellum with 36–53 segments, lateral flagellum with 26–42 segments. Male mesial flagellum longer than lateral flagellum, though only half as wide near basis (Fig. 5B). Mesial flagellum with about 80–90 sparsely setose segments; setae in males on average shorter compared to those on mesial flagellum in females. Proximal 3/4 of male lateral flagellum with 17–22 strongly swollen, setose segments; distal fourth with 13–16 normal segments; total of 30–38 segments. Basal segment strongly swollen with separate dorsal and ventral transverse stripes, proximally with comma-shaped stripes and distally with Y-shaped stripes, total of four stripes (Fig. 5B). Each stripe with coverage of long smooth setae. Distally adjoining 13–17 segments strongly swollen with separate dorsal and ventral, Y-shaped stripes, total of two stripes per segment, each again covered with setae (Fig. 5C). The 14–18 strongly swollen segments followed by transition zone of 3–5 segments with distally decreasing size and setae numbers, finally 13–16 normal segments. The sex-specific differences in setation and length of flagella weaker though also evident in subadults.

Antenna (Figs. 4A, B, 5F, G): sympod 3-segmented. Distolateral edge of terminal segment with strong tooth-like projection (dashed line in Fig. 5F). Distal third of antennal scale forms a setose lobe without spines. The large distalmost spine of the scale reaches to 0.2–0.5 times lobe length. Peduncle 3-segmented, whereby segments 1–3 contribute 15–18%, 40–43%, and 39–43% to total peduncle length. Basal segment of peduncle with strong tooth projecting near basis from mesial margin, and additional smaller tooth close to disto-mesial edge of this segment (solid line in Fig. 5F), no setae. Setae on median and terminal segments of peduncle on average longer in females than males. Antennal flagellum with moderate sexual dimorphism of segment numbers and setae structure. Flagellum with 41–46 well setose segments in females, versus 54–62 segments with fewer, on average shorter setae in males. Flagellum with only smooth setae in both sexes. However, normal setae strongly prevailing over shorter whip setae (Fig. 5G), the latter found only on basal sixth of the flagellum in females. By contrast, short whip setae prevail from segment 2 up to the apical segment in males. The sex-specific differences in setation and length of flagella weaker though also evident in subadults.

Foregut (Fig. 6): lateralia smooth over most of their surface; rostrally with short transverse series of 6–8 bilaterally serrated spines (Fig. 6F); mesially with longitudinal series of 9–11 (almost) unilaterally centro-apically serrated spines (Fig. 6B). Caudal parts of lateralia and dorsolateral infoldings with some apically coronate (pronged) spines (Fig. 6E). Dorsolateral infoldings on each side caudally with three unilaterally serrated spines (Fig. 6D), in part with secondary teeth; each side more rostrally with obliquely transverse series of 8–10 spines as in Fig. 6B; these series poorly visible (out of focus) in Fig. 6A. Superomedianum well setose, its lateral and caudal margins bearing numerous bilaterally centro-apically serrated spines (Fig. 6C).

Labrum (Fig. 7A): labrum roughly trapezoidal, rostrally weakly produced; ventral (= aboral) face flattened, dorsal (oral) face bulbous; mid-caudally densely setose, caudo-sub-medially to the right with short spines and to the left in addition with rugged surface facing the mandibles.

Mandibles (Fig. 5H–J): palp 42–49% carapace length; segments 1–3 contribute 7–10%, 58–63%, and 30–32% to total length, respectively. Palp (when stretched) anteriorly extend-

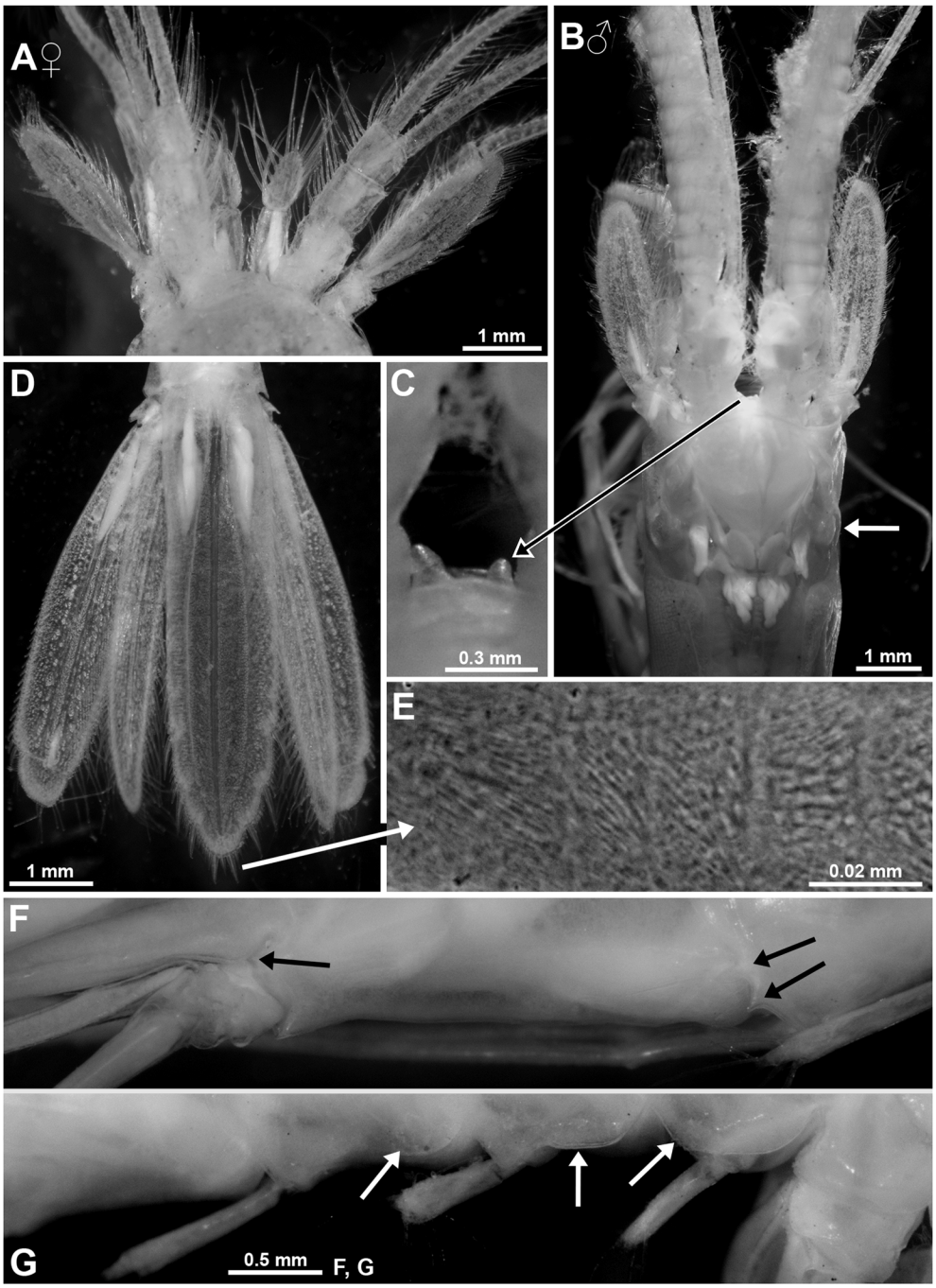

Fig. 4. *Hansenomysis pseudophthalma* sp. nov., holotype, adult female with BL 22.8 mm (F, G), paratypes, adult female 21.7 mm (A, E) and adult male 22.7 mm (B–D). A, anterior portion of female head, dorsal; B, anterior 2/3 of male cephalothorax, dorsal, short arrow points to eyelike hepatic bulge; C, detail of panel (B) showing processes of eye rudiment in front of anterior margin of carapace; D, tail fan, dorsal; E, detail of panel (D) showing scales on spine surface in another specimen, image turned anticlockwise; F, ventro-lateral portions of pleon-pleurite 6 and part of pleurite 5, paired arrows point to tooth-like caudal projections of pleurite 5, single arrow to scutellum paracaudale; G, ventro-lateral portions of pleon-pleurites 1–4, arrows point to up-tilted lower margin in pleurites 1–3.

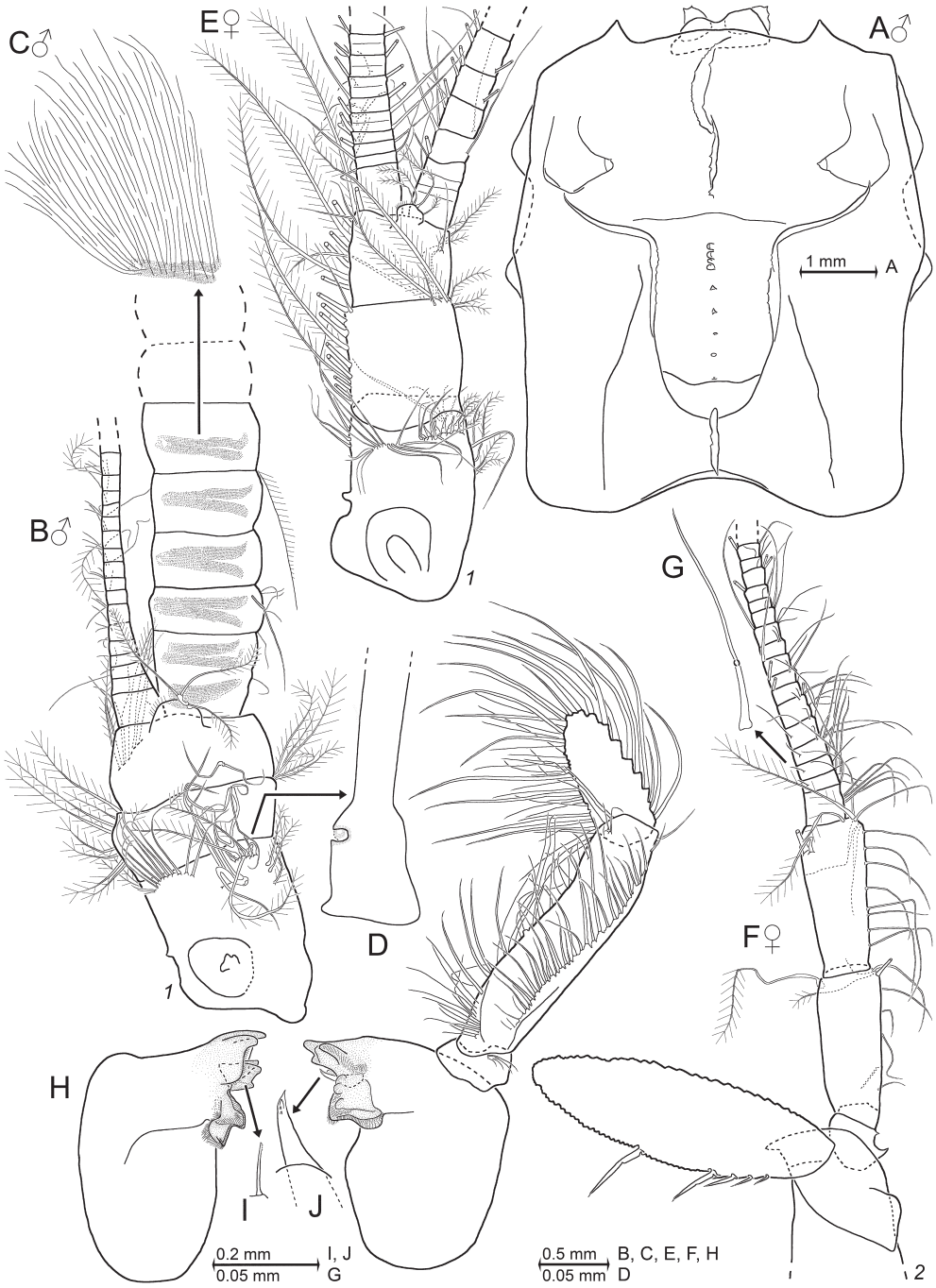

Fig. 5. *Hansenomysis pseudophthalma* sp. nov., paratypes, adult male with BL 22.7 mm (A–D, H–J) and adult female 21.7 mm (E–G). A, carapace with eye rudiment expanded on slide, dorsal; B, right male antennula, dorsal, transverse bands of setae on lateral flagellum indicated by setae bases only; C, detail of panel (B) showing dorsal transverse band of setae on lateral flagellum; D, detail of panel (B) showing indented basal portion of seta pertaining to group of setae (at blunt end of arrow) on basal segment of antennular trunk; E, right female antennula, dorsal; F, female antenna, dorsal, detail (G) shows whip seta of the flagellum; H, mandibles with right palpus, rostral, details show stylet (I) of left mandible and lacinia mobilis (J) of right mandible.

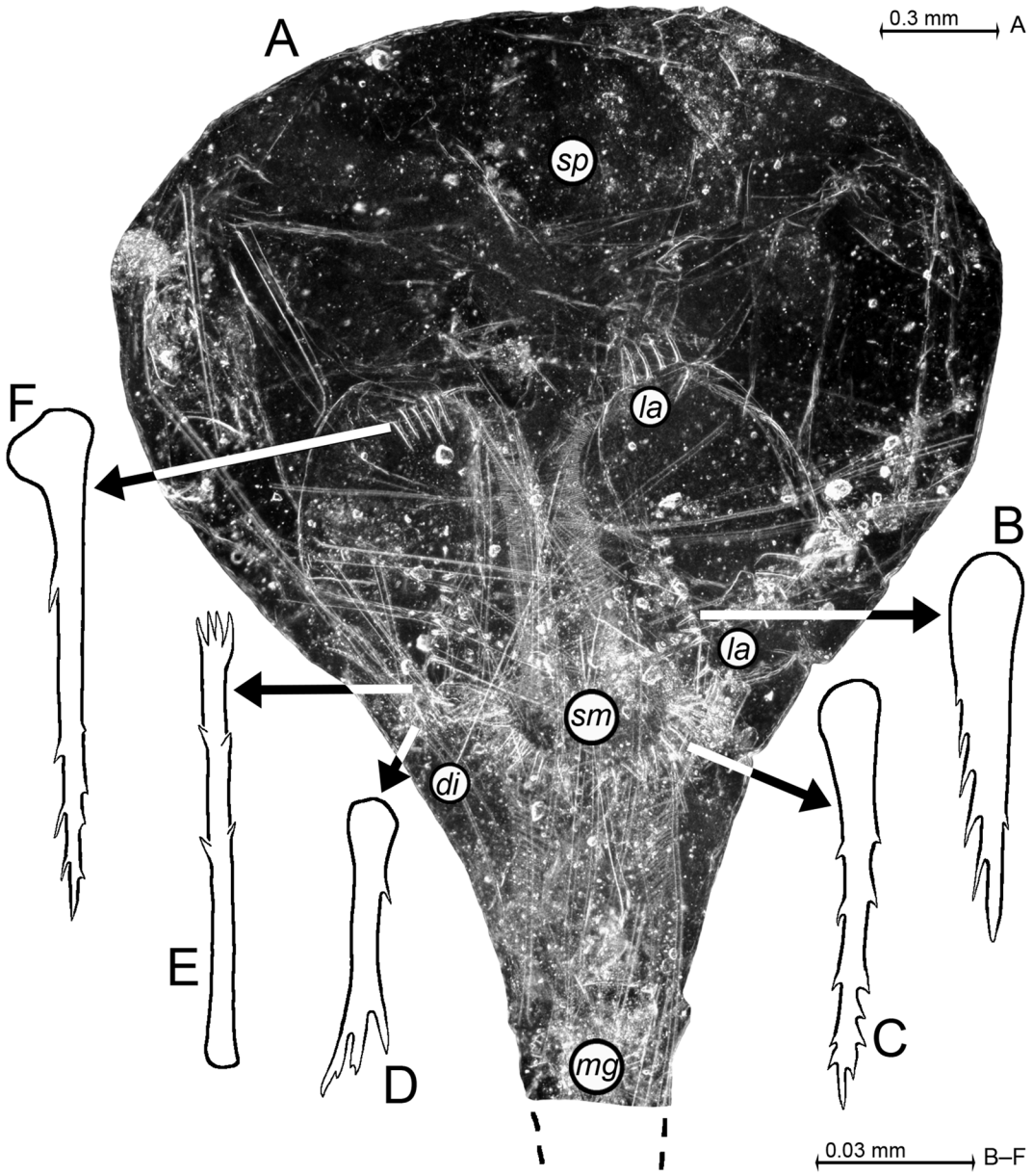

Fig. 6. Foregut in *Hansenomysis pseudophthalma* sp. nov., paratype, adult male with BL 22.7 mm. A, foregut expanded on slide, dorsal, lower case labels indicate dorsolateral infoldings (*di*), lateralia (*la*), midgut (*mg*), superomedianum (*sm*), and storage space (*sp*); B–F, details of panel (A), arrows point to diverse modified spines of the foregut.

ing to distal margin of median segment of antennular trunk (Fig. 4A) in female, beyond median segment of the shorter trunk in male. Basal segment of palp laterally with dense group of 4–7 short, smooth setae; median and distal segments setose all around; no spines, no teeth. Masticatory part of left mandible with large processus incisivus ending in three blunt teeth; lacinia mobilis well developed with four, mostly less blunt teeth; armature of the pars centralis reduced to a single, slender stylet (Fig. 5I). Right mandible with large processus

incisivus bearing four blunt teeth; lacinia mobilis reduced to a basally wide spine bearing minute apical teeth (Fig. 5J); pars centralis bare. Left and right processus molaris bilobate; both lobes sclerotized, proximal lobe with ventral and dorsal ridges bearing stiff bristles.

Labium (Fig. 7B): labium normal, bilobate. Inner face of lobes distally with dense series of stiff bristles. Inner face with short but strong spines on bulge projecting at 1/3 to 1/2 length from basis.

Maxillula (Fig. 7C): distal segment shorter than exopod of maxilla. This segment terminally with 12–14 large smooth spines. Four barbed setae in transverse series shortly proximally from the spines, no pores visible. Endite subterminally with three large setae bilaterally bearing short barbs along basal 3/4, distal fourth unilaterally microserrated by minute stiff barbs. Endite disto-ventrally (= aborally) with basally barbed 0–1 seta, and dorsally (= orally) with series of five smooth setae distally increasing in length.

Maxilla (Fig. 7D): sympod 2-segmented with three strongly setose endites. Palp with two stout segments, the distal segment contributing 60–70% to total length, its length 0.7–0.9 times maximum width. Distal segment setose all around, basal segment with only 6–7 barbed setae on mesial margin. Exopod comparatively slender, length 2.4–2.8 times maximum width; exopod reaches to mid of distal segment of palp; exopod densely furnished with plumose setae all along outer margin, only 3–4 setae most distally on mesial margin; part of mesial margin with dense series of minute hairs.

Thoracopods in general (Fig. 7E–L): total length of exopods as well as their flagella increases from exopods 2 to (5–6), and then remains subequal up to exopod 8. Both sexes with basal plates rounded at distolateral edge and with well setose flagella. Plates slender, lateral margins parallel, length about three times width in exopods 2–8 of females (Fig. 7G) and in exopods 2, 3 of males. Plate of male exopods 4–8 with distally weakly diverging margins; length only about two times average width. Flagellum of exopods 2–8 with 8–9, 9, 9, 10, 10, 11, and 11 segments in males, and 8, 8, 8–9, 9, 9, 9, and 9 segments in females, respectively. Endopod length strongly increasing from 0.4 times carapace length in endopod 1 up to 1.2–1.3 in endopod 6 and then slightly decreasing to 1.0–1.1 in endopod 8.

First thoracopod (maxilliped 1, Fig. 7E, F): well-developed endopod and epipod (Fig. 7E), no exopod. Epipod long, slender, smooth all around, scaphocerite-like. Endopod strong, robust, most setae implanted on inner face from basis to dactylus; merus with short, weak endite, carpus and propodus each with strong endite. Dactylus with four strong, spine-like setae (Fig. 7F) that are bilaterally rugged due to cover of minute, stiff, acute bristles; dactylus without nail. Endites of carpus and propodus each with three such spine-like setae. Endite of merus with longitudinal series of 6–7 much smaller setae of that kind; those setae increasing in length distally.

Second thoracopod (maxilliped 2; Fig. 7G): endopod robust, somewhat longer than that of first thoracopod. Praeischium small, simple, smooth. Inner face of ischium with very large, broadly linguiform endite with length about 2.3–2.8 times maximum width, endite distally projecting up to 0.6–0.7 times merus length (upon about parallel alignment); mesial and terminal margins of endite all along densely occupied by smooth setae; lateral margin with 5–8 shorter such setae. Merus sub-quadrangular, its length three times maximum width; mostly smooth setae along inner margin, subterminally with additional 6–7 densely set, unilaterally spiny, short setae; only one small smooth seta distally on outer margin. Carpopropodus mesially swollen, length 1.6–1.9 times maximum width, numerous long setae in lateral portions, less in mesial portions, mesial margin with median group of 5–8, densely set, unilaterally spiny setae (as on merus). Dactylus

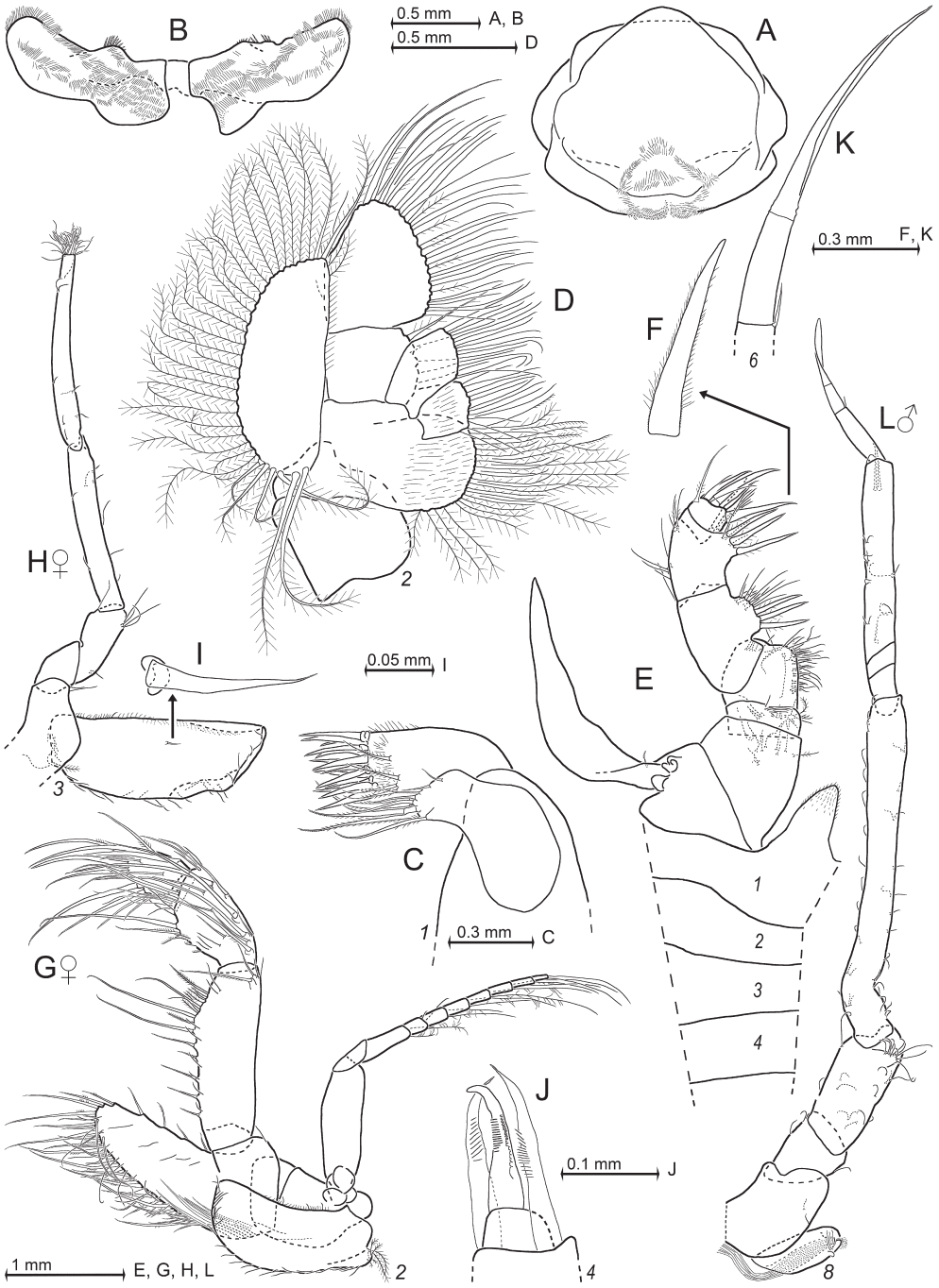

Fig. 7. *Hansenomysis pseudophthalma* sp. nov., paratypes, adult male with BL 22.7 mm (A–C, E, F, J–L) and adult female 21.7 mm (D, G–I). A, labrum, obliquely ventral (= aboral); B, labium, caudal; C, maxillula, caudal; D, maxilla, caudal; E, thoracic endopod 1 with epipod (caudal) and sternites 1–4 (ventral), detail (F) shows modified spine-like seta from dactylus; G, thoracopod 2 (caudal) including its (somewhat displaced) oostegite; H, thoracic endopod 3 with oostegite 2, lateral, detail (I) shows spine-like seta on outer face of oostegite; J, tip of thoracic endopod 4, dactylus with claw and paradactylary setae, other setae omitted, mesial aspect; K, dactylus 6, lateral; L, thoracic endopod 8 (rostral) with penis (lateral).

strong, bearing dense brush of long setae, no nail. Part of large setae on carpopropodus and dactylus bilaterally armed with short acute bristles as in Fig. 7F.

Third to fifth thoracopods (Figs. 7H, I, 11B, G): endopods 1.5–1.9 times length of exopods. Meri 3–5 are 0.3–0.4 times endopod length measured from praeischium to dactylus. Endopod with praeischium 0.2–0.4, ischium 0.2–0.4, carpopropodus 1.0–1.2, and dactylus 0.02–0.04 times length of merus, each element not subdivided (Fig. 7H). The here reported size relations take into account that praeischium and ischium overlap due to their oblique articulation. Merus and carpopropodus unsegmented in both sexes. Setation of dactylus and of terminal margin of propodus together contributing to a dense brush of setae (Figs. 7H, 11B) covering short 'serrated' claw and two paradactylary setae (Figs. 7J, 11G).

Sixth to eighth thoracopods (Figs. 7K, L, 11L, Q): endopods 1.7–2.2 times length of exopods. Meri 6–8 measure 0.4 times endopod length measured from praeischium to dactylus. Endopods with praeischium 0.1–0.2, ischium 0.3–0.4, carpus 0.7–0.8, propodus 0.2, and dactylus 0.1 times length of merus. Only males with 2-segmented merus 6, 7; segments separated by a slightly oblique articulation, basal segment 0.3 times total merus length. Meri 6–8 in females and merus 8 in males unsegmented. Carpi 6–8 with three segments separated by oblique articulations in both sexes, the two basal segments each with only one-tenth total carpus length. Propodus with small smooth seta at mesial edge with the dactylus (Figs. 7K, 11L).

Penes (Fig. 7L): penes not extending beyond basis of thoracic endopod 8. Penes tube-like, terminally bilobate, well rounded; subterminally with small smooth seta. Series of minute stiff bristles along distal circumference of lobe facing the ejaculatory opening.

Marsupium (Fig. 7G–I): brood pouch formed by seven pairs of oostegites emerging from thoracopods 2–8. Size of oostegites increasing caudally; ultimate oostegite about 1.8 times as long as first oostegite. Upper margin of oostegites straight to slightly concave, bearing almost all along small smooth setae; proximal half of this margin in addition with dense series of tiny hairs positioned between the smooth setae. Well-rounded lower margin all along with larger smooth setae. Proximal margin with even longer barbed setae. Oostegites 2–7 (from thoracopods 3–8) each with one spine-like seta (Fig. 7I) on outer face, no such seta in oostegite 1 (Fig. 7G). One of two dissected oostegites 4 with an additional closely set seta of that kind. These setae *in loco* invariantly projecting perpendicularly away from their oostegite (seta artificially forced into slide plane in Fig. 7H). A few additional slender smooth setae on outer face of oostegites 3–7.

Pleon (Figs. 4F, G, 8A–I): pleomeres 1–5 measure 0.5–0.7, 0.4–0.6, 0.5–0.6, 0.6–0.7, and 0.7–0.8 times length of pleomere 6. Pleurites 1–3 with up-tilted lower margins (arrows in Fig. 4G). For tooth-like protrusions of pleomeres see above diagnosis. Female pleopods (Fig. 8A–C) increasing in length caudally, with strongest increment between pleopods 4 and 5; pleopod 5 extending beyond pleomere 6. Female pleopods with most setae positioned on distal third. These setae with smooth proximal half and barbed distal third to half. Similar numbers of such setae also present on distal two segments of endopod of male pleopod 5 (Fig. 8I), and on basal 3–4 segments of male endopods 2–4 (Fig. 8F, H), fewer setae on male endopod 1 (Fig. 8D). A few such setae also present on antennular trunk, antennal peduncle, and terminal segment of exopod of uropods in both sexes. Male pleopods 1–5 with 14-, 15–16-, 15-, 16-, 15-segmented exopods and with 1-, 14–15-, 15-, 16-, 3-segmented endopods, respectively (Fig. 8D, F, H, I). Length of male exopods subequal, whereas size strongly increasing between endopods 1 and 2, and then weakly in series of endopods 2–5; endopod of

the biramous male pleopod 5 (Fig. 8I) most similar to the uniramous female pleopod 5 (Fig. 8C), also extending beyond pleomere 6. Male pleopods show a greater diversity of setae: plumose setae prevail on exopods 1–5 and endopods 2–4. Incidence of distally barbed setae as indicated above. In addition, there are more strongly modified setae, namely basally wide, subapically spinose setae (Fig. 8E) on endopod 1; and more slender, subbasally to apically spinose setae (Fig. 8G), one seta on each of basal five segments of exopod 2. These five setae measuring 3–6 times length of segment 3.

Uropods (Figs. 4D, 8J, K): endopod slender; length 7–8 times maximum width; mesial margin straight to slightly concave, lateral margin convex. Exopod 0.9–1.0 times as long as endopod (Figs. 4D, 8J). Total length of exopod five times maximum width, basal segment 9/10 total length and 1.4–1.8 times broader than apical segment. Apical segment densely equipped with plumose setae, only lateral margin additionally bearing a few small, distally barbed setae (Fig. 8K).

Telson (Figs. 2A, B, 4D, E, 8L): telson twice as long as ultimate pleomere, extending 4–12% its length beyond endopod and 9–16% beyond exopod of uropods (Fig. 2A, B). Cross section showed up-tilted lateral margins along major part of telson. Accordingly, apparent width increased considerably by forcing the telson into a plane through pressure exerted by the cover glass (Fig. 4D versus 8L). Distal third of lateral margins converging in four convex partitions, each delimited by large spines. Terminus with pair of large submedio-apical spines flanking a medio-apical spine with 0.6–0.7 times their length. Distal spines are hispid all around due to cover of minute spine-like scales densely set on transverse stripes (Fig. 4E). Coverage decreases with decreasing size of spines and with increasing distance from terminus of telson. Proximal half of telson with smooth spines only.

Gut contents.—Foreguts of both dissected adults contain large numbers of broken molts of long plumose setae (Fig. 6A). Native setae of that kind are present on antennal scale and uropods. Thus it appears plausible that the two specimens had fed on their own exuviae. Remaining components are masticated, unidentifiable organic material and mineral particles. Storage volume filled to 60% in female with BL 21.7 mm, only ＜5% in the figured (6A) male with 22.7 mm.

Hansenomysis sorbei San Vicente, 2009
Figs. 9, 11C, H, M, R

Hansenomysis sorbei San Vicente, 2009: 31–39, Figs. 1–5 (first description); Mees & Meland, 2022: AphiaID 431973 (accepted).

Material.—Powell Basin: 2 ♀♀ adult, BL 23.3–23.9 mm, 4 juv. 7.9–9.3 mm, #III-133-2, 62.7748°S 53.0583°W to 62.7730°S 53.0663°W, 1584–1579 m, 16 Mar. 2005, epinet; 1 ♀ imm. 16.2 mm, recovered from sediment in web mug, same haul as before.

Diagnosis.—Based on adult females only. All female features of generic diagnosis. Eye rudiment not or shortly projecting beyond anterior margin of carapace; rudiment with pair of small, triangular to tooth-like, paramedian processes, and with pair of yet smaller, rounded lateral processes. Carapace (Fig. 9) with rounded anterior margin, no rostrum. Its cephalic region with short longitudinal gastric carina (Fig. 9A) and with three pairs of calotte-shaped bulges (Fig. 9A, C), among these only the hepatic bulges with tooth-like projection (Fig. 9B). Pair of submedian longitudinal crests with one-fifth carapace length start shortly behind cervical sulcus (Fig. 9C). More laterally and caudally, starting at 3/5 carapace length from anterior margin, a pair of large, weakly converging keels runs caudally to about one-twentieths carapace length in front of the

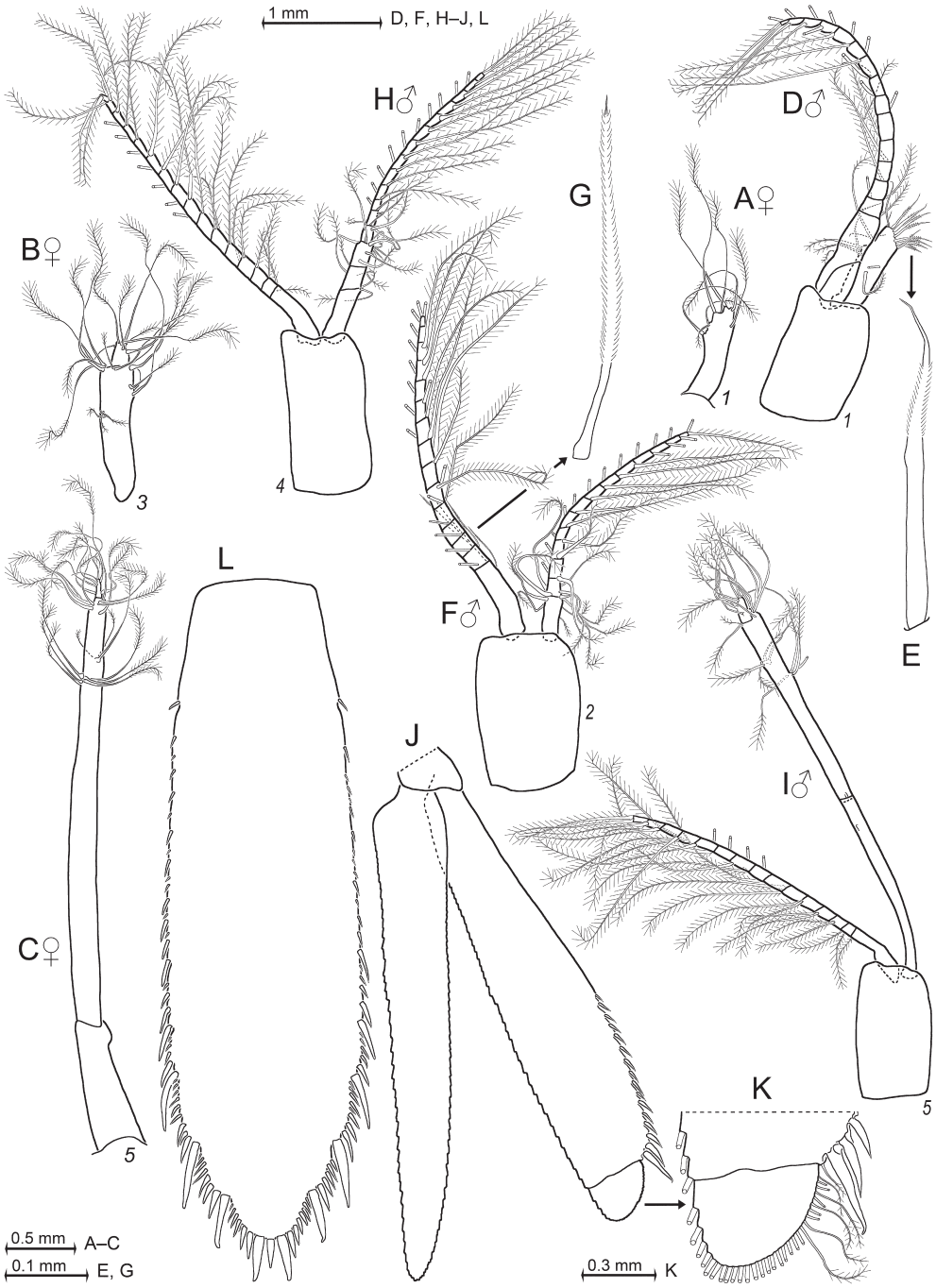

Fig. 8. Pleopods and tail fan in *Hansenomysis pseudophthalma* sp. nov., paratypes, adult female with BL 21.7 mm (A–C, J, K) and adult male 22.7 mm (D–I, L). A–C, series of female pleopods 1, 3, 5; D, left male pleopod 1, detail (E) shows modified seta of endopod; F, left male pleopod 2, detail (G) shows modified seta of exopod; H, I, left male pleopods 4, 5; J, uropods, dorsal, detail (K) shows distal portion of exopod; L, telson expanded on slide.

posterior margin. The keels flank a longitudinal median crest with one-sixth carapace length. This crest ends very close to posterior margin of carapace. Antennal scale 5–6 times longer than wide, extending 0.1–0.2 times its length beyond antennal peduncle and 0.3–0.7 beyond antennular trunk. Proximal 10–30% of antennal scale with smooth outer margin, median 35–45% with 5–8 spines distally increasing in size; distal 35–45% occupied by setose lobe without spines. Distal three spines with setae in between; distalmost spine not reaching to mid of apical lobe. Thoracomeres 7, 8 with dorsally up-tilted anterior margin. Posterior margin of pleomeres 4–6 each produced in a total of 5–7 strong teeth; mid-dorsal tooth strongest, flanked on each side by one sublateral and 1–2 smaller lateral teeth. Pleomere 3 with total of only three such teeth, pleomeres 1, 2 without any. Female pleopods 1–4 unsegmented; pleopod 5 longest, 3–4-segmented, not extending beyond pleomere 6. Both rami of uropods subequal, reaching to about terminus of telson. Proximal segment of exopod of uropods with smooth outer margin along proximal third. Distal 2/3 of margin with 22–26 spines discontinuously increasing in length distally. Distalmost spine not extending beyond setose apical segment. Telson linguiform, four times as long as wide, proximal 2/3 of lateral margins slightly converging (almost parallel), distal third distinctly converging to broadly rounded, convex terminus. Proximal third of lateral margins with subequal, short spines; distal 2/3 with discontinuous series of long spines with shorter spines in between; distalmost large lateral spines extending beyond the terminal margin. Terminal margin with two large spines in alternating series with 1–3 intermediate-sized spines.

Descriptive notes.—Both available adult females show patterns of teeth on posterior margins of pleomeres as in the above diagnosis. Immature with weaker dorsal and sublateral teeth, no lateral teeth on pleomere 6; totals of only one or three teeth on pleomeres 4, 5, respectively. The terminal spines of the telson hispid along their proximal portions. For structure of carapace and thoracic endopods see also chapter 'Morphological Account' below.

Distribution.—Type locality in the Bellingshausen Sea, 70.2372°S 81.7686°W; sample taken with suprabenthic sledge in 1869 m depth (San Vicente 2009). The new record taken with an epibenthic sledge in 1584–1579 m depth extends the known geographical range to the Powell Basin at 62.7730°S 53.0663°W.

Hansenomysis anaramosae San Vicente & Sorbe, 2008
Figs. 10A, B, D–G, 11E, J, O, T

Hansenomysis anaramosae San Vicente & Sorbe, 2008: 1439, Figs. 1–8 (first description); San Vicente, 2010: 37, Fig. 21 (diagnosis, distribution, in key); Petryashov, 2014: 5.16: p. 150 (biogeography); Mees & Meland, 2022: AphiaID 432377 (accepted).

Material.—Weddell Sea: 1 imm., BL 13.9 mm, 1 juv. 7.7 mm, #II-132-2, 65.2957°S 53.3803°W to 65.2927°S 53.3805°W, 2086 m, 6 Mar. 2002, epinet; 1 juv. 6.4 mm, same sampling data as before, supranet; 1 ♂ ad. 29.7 mm, 1 ♀ subad. 27.7 mm, 1 imm. 14.1 mm, #II-133-3, 65.3358°S 54.2392°W to 65.3343°S 54.2418°W, 1122–1119 m, 7 Mar. 2002, epinet; 1 juv. 7.2 mm in separate vial, same sampling data as before, supranet; 1 ♀ imm. 15.7 mm, 5 juv. 6.7–10.0 mm, #III-074-6, 71.30583°S 13.96183°W to 71.30467°S 13.95517°W, 1030–1040 m, 20 Feb. 2005, epinet.

Diagnosis.—Based on adult male and on subadults of both sexes. All respective features of generic diagnosis. Eye rudiment with pair of horn-like to triangular paramedian processes and a pair of short rounded lateral processes (Fig. 10B, F, G), no visual elements. Antennal

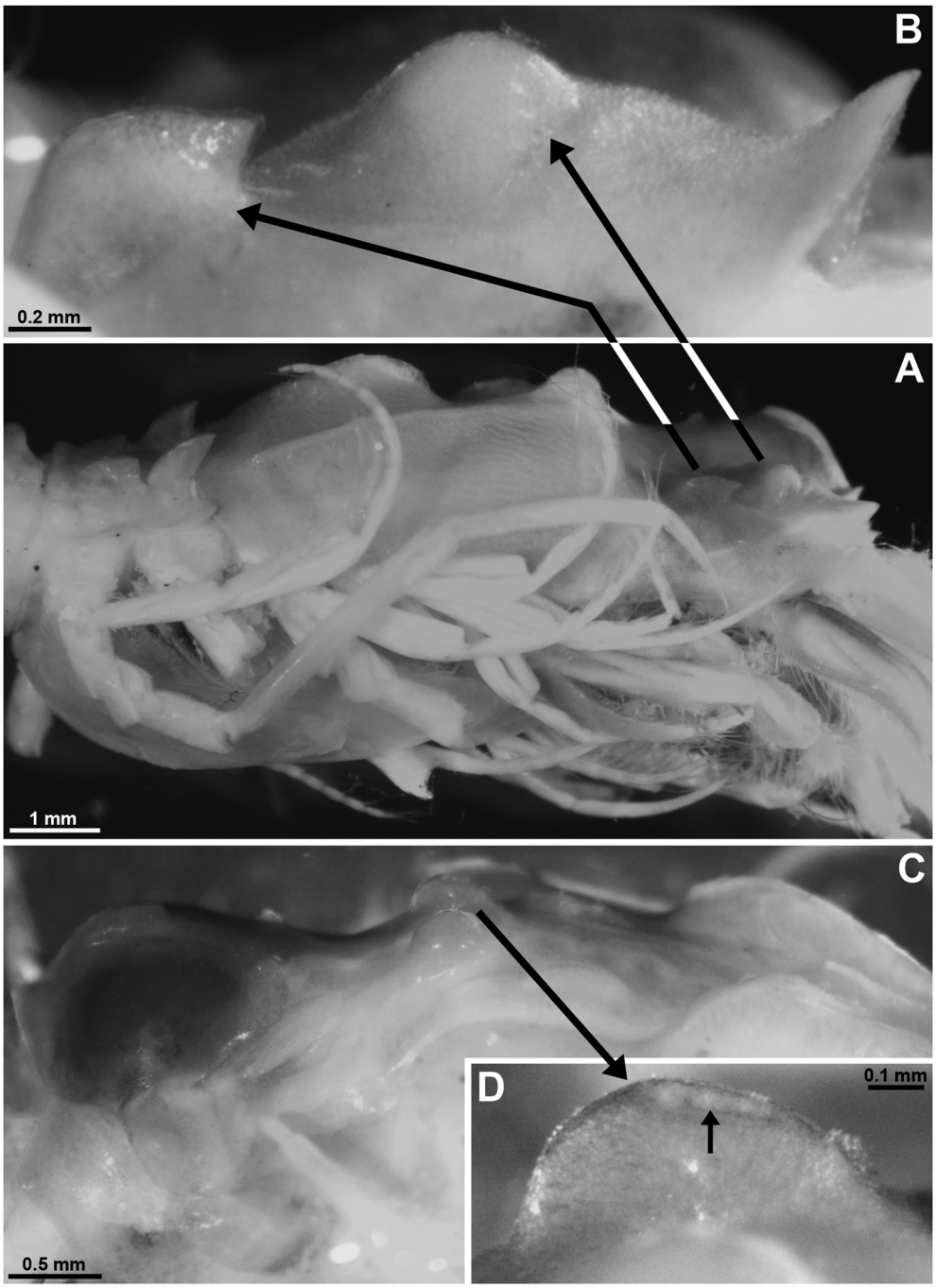

Fig. 9. Cephalothorax and bulges of the carapace in *Hansenomysis sorbei* San Vicente, 2009, adult female with BL 23.9 mm. A, cephalothorax, right latero-ventral aspect; B, slightly more inclined detail of panel (A) showing hepatic (left arrow) and antero-lateral (right arrow) bulges; C, cephalothorax, left lateral aspect; D, detail of panel (C) showing right, paramedian cervical bulge.

scale of adult male reaching 12–21% its length beyond antennal peduncle and 39–55% beyond antennular trunk. Proximal 15–20% of antennal scale with smooth outer margin, median 51–54% with 14–17 spines distally increasing in size, no setae between spines. Distal 30–34% of antennal scale forms a setose lobe without spines. Distalmost spine not reaching to terminus of lobe. Carapace with short triangular rostrum (Fig. 10G; out of focus in 10B); disto-sublaterally produced in large acute teeth, distolateral edges well rounded. Cephalic region of carapace with short, triangular gastric carina (Fig. 10E, G), with three teeth along midline and two pairs of teeth in lateral position. Posterior to the cervical sulcus, two large longitudinal, sublateral keels running backwards and meeting together in a 'U'-shaped manner. Each keel with an anterior and a mesial tooth. An additional unpaired tooth at the median meeting point of the large keels. Thoracomeres 6–8 with dorsally up-tilted anterior margin, most strongly so in thoracomere 6. Lateral tooth-like projections on anterior margin of thoracomeres 7, 8. Pleomeres 1–5 without spines or teeth, pleomere 6 laterally with two pairs of tooth-like projections from the terminal margin. Female pleopods 1–4 unsegmented; pleopod 5 long, 2–3-segmented, extending beyond pleomere 6. Male pleopods biramous; endopods 2–4 and all exopods multisegmented; endopod 1 unsegmented; endopod 5 rod-like, up to 3-segmented, most similar to uniramous pleopod 5 of the female, also extending beyond pleomere 6. Lateral margin of basal segment of exopod of uropods with smooth basal third; distal 2/3 with 18–27 densely set spines in series of intermediate-sized spines with smaller spines in between. The large distalmost spine shorter than the setose terminal segment. No setae on lateral margin of the basal segment except for one seta at the edge with the terminal segment. Telson 3–4 times as long as wide, proximal 2/3 with parallel margins, distal third V-shaped, converging to a narrow, transversely truncate apex. Proximal sixth to seventh of telson with smooth margins; distally following portions with series of large spines with small spines in between. Distalmost and penultimate large lateral spines each about one-seventh telson length, only distalmost large spine extending beyond the telson apex. Apical margin with one pair of large distolateral spines flanking a smaller median spine. Telson extending 13–19% its length beyond both rami of uropods.

Morphological notes.—The very well-preserved adult male with tube-like, simple, short penes, extending to proximal margin of praeischium of thoracic endopod 8. Endopods of male pleopods 1–5 with 1, 16, 18, 13, 3 segments, exopods with 18, 18, 18, 18, 17 segments, respectively (see Discussion). Pleomere 6 with scutellum paracaudale ending in a strong tooth. Disto-latero-ventral edge of pleomere 6 with tooth-like posterior extension (in front of uropods). Antennal scale 4–6 times as long as wide in specimens with BL exceeding 13 mm. For eye development, structure of carapace and thoracic endopods see chapter 'Morphological Account' below.

Occurrence.—Type locality in Bellingshausen Sea, 70.2450°S 81.7683°W, suprabenthic in 540 m depth. In this sea also taken at 70°S 78°W, 1083 m depth (San Vicente & Sorbe 2008). Present material taken from a total of five samples in the NW-Weddell Sea at 65°S 53–54°W and in the SE-Weddell Sea at 71°S 14°W, depth range 1030–2086 m, in the epinet and supranet of epibenthic sledges.

Hansenomysis angusticauda O. S. Tattersall, 1961
Fig. 11D, I, N, S

Selected references:

Hansenomysis antarctica, O. S. Tattersall, 1955: 59, Fig. 8 (record, description).

Hansenomysis angusticauda O. S. Tattersall, 1961: 559–565, Figs. 3–10 (diagnosis,

description); Petryashov, 2005: 962, Fig. 3 (records, distribution, in key); San Vicente, 2010: 36 (diagnosis, distribution, in key); Wittmann, 2013: Tab. 1, Figs. 1e, 3a (record, male sexual characteristics); Petryashov, 2014: 150 (biogeography); Mees & Meland, 2022: AphiaID 226224 (accepted).

Material.—South Shetland area: 1 ♀ subad., BL 28.2 mm, #I-046-7, 60.6392°S 53.9560°W to 60.6353°S 53.9582°W, 2893.6–2893.2 m, 30 Jan. 2002, epinet.

Diagnosis.—Based on subadult females and adult males. All respective features of generic diagnosis. Transverse eye rudiment with pair of horn-like to triangular paramedian processes, and a pair of short, broadly rounded, lateral processes (see Discussion), no visual elements. Antennal scale 4–5 times as long as wide, reaching 15–23% its length beyond antennal peduncle and 25–45% beyond antennular trunk. Proximal fourth of the antennal scale with smooth outer margin, median half with 13–22 spines distally increasing in size, no setae between spines. Distal fourth of antennal scale forms a setose lobe without spines. Carapace with continuously rounded disto-median margin, disto-sublaterally produced in large, acute, tooth-like projections, distolateral edge well rounded. Its cephalic region with short longitudinal gastric carina; with three teeth along midline, and laterally with one pair of hepatic teeth. Posterior to the cervical sulcus two large longitudinal, sublateral keels running backwards and meeting together in a 'U'-shaped manner. Each keel with an anterior and a mesial tooth. An additional unpaired tooth at the median meeting point of the large keels. Pleomeres 1–5 without spines or teeth, pleomere 6 on each side with two tooth-like projections from the terminal margin, among which a large triangular tooth contributed by the scutellum paracaudale. Female pleopods 1–4 unsegmented; pleopod 5 long, 3-segmented, extending beyond pleomere 6. Male pleopods biramous; endopod 1 unsegmented; endopods 2–4 and all exopods multisegmented; endopod 5 rod-like, 3-segmented, most similar to uniramous pleopod 5 of female, also extending beyond pleomere 6. Lateral margin of basal segment of exopod of uropods with smooth basal 2/5 of its length, dense series of 21–39 spines along distal 3/5; no setae on lateral margin except for one seta at the edge with the terminal segment. Lateral margin with series of intermediate-sized spines with smaller spines in between. The large distalmost spine shorter than the setose apical segment. Telson 4–5 times as long as wide, proximal 2/3 to 3/4 with parallel margins; remaining distal portion V-shaped, converging to a narrowly blunt apex. Proximal ≤10% with smooth lateral margins; distal portions all along with series of large spines with small spines in between. Penultimate and ultimate, large lateral spines 9–14% and 4–10% telson length, respectively, ultimate spine in part reaching to the apex of the telson, while not so the penultimate one. Apex with one pair of large distolateral spines flanking 0–1 smaller median spine. Telson extends 0.1–0.3 times its length beyond both rami of uropods.

Morphological notes.—Penes as described by Wittmann (2013), coinciding with the above description of *H. pseudophthalma* sp. nov. For structure of carapace and thoracic endopods see chapter 'Morphological Account' below.

Occurrence.—Type locality is the Ross Sea, 75.25°S 165.92°E; types sampled with non-closing net towed from 808 m depth to surface (O. S. Tattersall 1961). Species previously known from Antarctic Peninsula, Weddell Sea and Ross Sea, 61°S–75°S, pelagic and suprabenthic in 160–1280 m depth (Petryashov 2005, San Vicente 2010, Wittmann 2013). The present subadult female taken with epinet mounted on self-closing epibenthic sledge, NE of Elephant Island, 62°S 54°W, depth 2893 m, yielding a strong vertical range extension.

Morphological Account

Notes on eye structure and development.—Three species from the ANDEEP samples, namely *Hansenomysis anaramosae*, *H. angusticauda* and *H. sorbei*, show a pair of paramedian, rostral eye processes, and a pair of smaller, rostrally projecting lateral processes (Fig. 10B, F, G), total of four processes per species. Only the lateral processes but no paramedian processes found in *H. chini* and *H. pseudophthalma* sp. nov.

The same basic mode of post-larval eye development is reported here in *Hansenomysis anaramosae* (Fig. 10A, B, D–G), *H. chini* (Fig. 10C), and *H. pseudophthalma* sp. nov. The juveniles start with two at least rostrally separate bulbs (Fig. 10A) inside a common cutícular sheath forming a transverse bar, swollen externally at the position of the bulbs, no visual elements. In lateral view the swellings are calotte-shaped to varying (species-specific) degrees, feigning well-developed eyes (Fig. 10D). The compound organ forms a bar with bulbs rather than an eyeplate. Eye processes are represented by short anterior protrusions at this stage of development. During further development the eye rudiments retreat to varying (species-specific) degrees (Fig. 10B) under the anterior margin of the carapace (Fig. 10C) or not so; the processes become longer, and the bulbs flatten, although a bulb-like formation persists until the adult stage (Fig. 10F, G). Not considering the processes, the dorsoventral extension of the eye rudiment surpasses the antero-posterior extension in adults.

Structure of carapace.—*Hansenomysis anaramosae* and *H. angusticauda* share large hepatic teeth; no eyelike structures were visible in all stages available. Carapace with large keels and furrows, and a number of teeth. Additional details in the above diagnoses of these species.

Hansenomysis chini (Fig. 1A, B): calotte-shaped bulge without teeth present in the hepatic region, where teeth are present in many other species. Tooth-like structure close to the bulge is feigned by an accidental fold in Fig. 1A. No such 'tooth' on opposite side of this specimen; also not found anywhere in both subadult specimens available. Bulge diameter is about 2% body size in (sub)-adults. Bulge very low, weakly apparent in juveniles. Relative height of bulge increases with increasing body size. Bulge elevated by about a third of its diameter in the adult female. Only in the adult the outer circumference of the bulge shows a shell of centripetal lamellae (interpreted as photocytes as detailed for *H. pseudophthalma* in Fig. 3E), this makes the bulges feign eyes (Fig. 1B, see Discussion). Additional details of the carapace in the above diagnosis of this species.

Hansenomysis pseudophthalma sp. nov. (Figs. 3, 4B): hepatic bulges calotte-shaped with height 1/3 to 2/3 width at basis, diameter about 2% body size in adults. Bulges bearing obliquely anteriorly facing, comparatively large teeth in non-adults (Fig. 3D). The large teeth of immatures accompanied by small disc (labeled '*rph*' in Fig. 3D), the latter interpreted as rudiment of photophore with photocytes and lacunary system not yet visible. Bulges and discs become larger while the teeth become relatively smaller or disappear with increasing body size (series of panels D, C, B in Fig. 3). Structure and brown color contrast from the carapace and contribute to the outward appearance of the bulges as eyes in adults (Fig. 3A, B; less striking in Fig. 3C). Outer face of mature bulges with subcuticular layer of large cells, visible as reticulate pattern in Fig. 3B. Bulges in adults of both sexes apically bearing a disk- to calotte-shaped photophore facing obliquely anteriorly (Fig. 3A). Mature photophores with lens, photocytes, lacunary system, basement membrane, and nerve fibers as detailed in Fig. 3E. Photocytes epidermal, not integrated in hepatic caeca. These luminescent organs

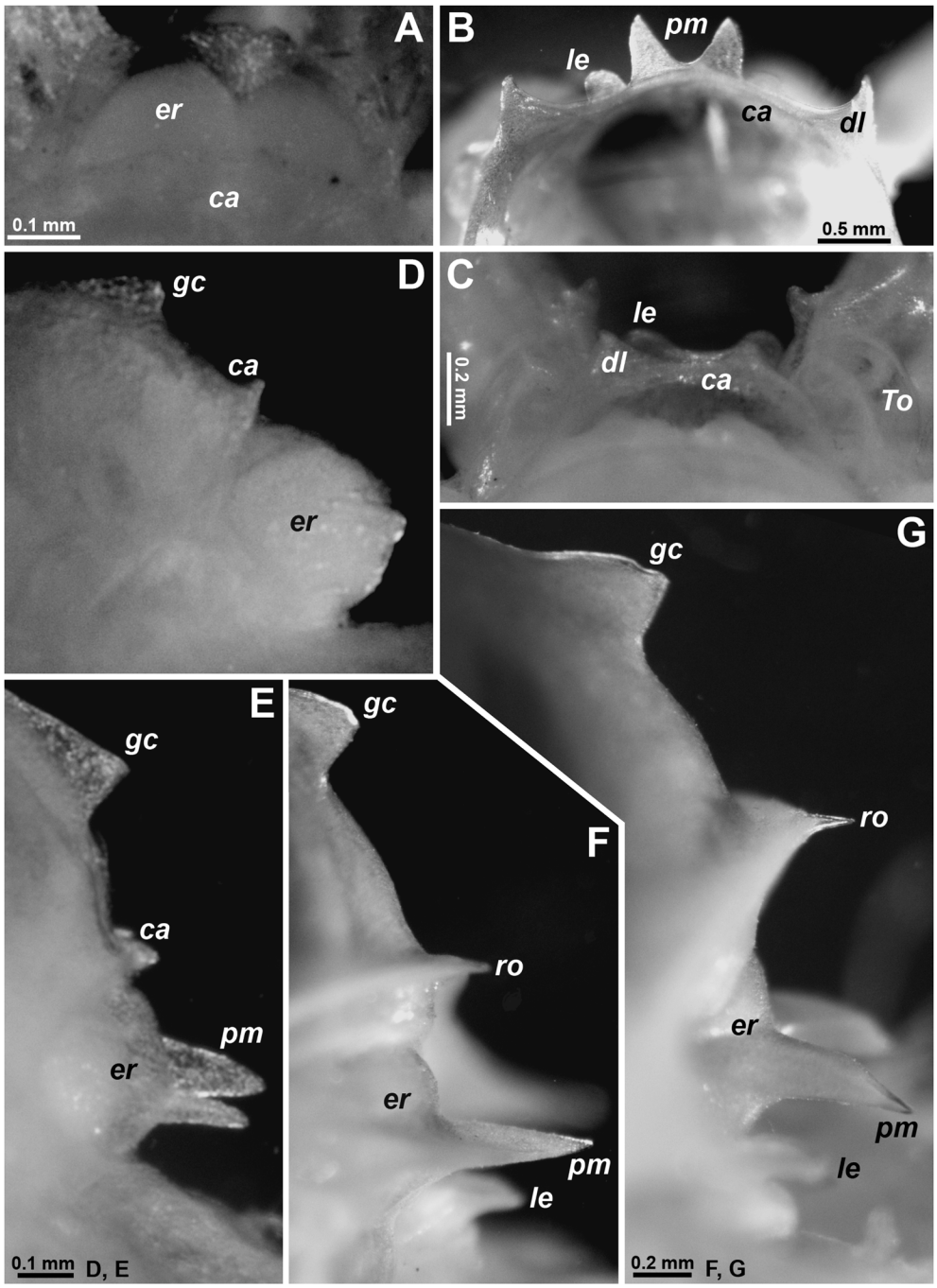

Fig. 10. Structure and post-larval development of eye rudiment in *Hansenomysis anaramosae* (A, B, D–G) and *Hansenomysis chini* (C). A–C, dorsal aspect of eye rudiment in front of carapace in juvenile with BL 6.4 mm (A), immature 15.7 mm (B), and adult female 16.3 mm (C). D–G, lateral aspect of frons with eye rudiment and anterior margin of carapace in juvenile 6.7 mm (D), juvenile 10.0 mm (E), subadult female 27.7 mm (F), and adult male 29.7 mm (G). Labels indicate carapace (*ca*), distolateral process of carapace (*dl*), eye rudiment (*er*), gastric carina (*gc*), lateral eye process (*le*), paramedian eye process (*pm*), rostrum (*ro*), and Tattersall organ (*To*).

nearly same-sized and very similar to the photophores described by Terao (1917: Fig. 1) for a sergestid decapod. Additional details of the carapace in the above diagnosis of *H. pseudophthalma* and in the Discussion.

Hansenomysis sorbei (Fig. 9): cephalic portion of carapace with total of three bulges on each side (Fig. 9A, C). Height and calotte-like shape of these bulges increase with increasing body size. Hepatic bulge (left arrow in Fig. 9A, B) with distinct, anteriorly projecting tooth in all stages available. Relative size of this tooth decreases weakly with increasing body size, nonetheless, teeth are still well-developed in adult females. An additional, smooth bulge (right arrow in Fig. 9A, B) set closely in front of the hepatic bulge. Directly in front of the cervical sulcus, a pair of larger bulges (Fig. 9C) closely flanks the midline of the carapace; bulge diameter about 3% body size in adults. Bulges of this third pair show smooth cuticle over most of their surface, and a reticulate pattern of large cells is visible below the cuticle. Distally these bulges bear hyaline cuticle in a delimited, circular area facing upwards (Fig. 9D). Additional details on carapace in the above diagnosis of this species and in the Discussion.

Structure of thoracic endopods.—All here examined *Hansenomysis* species, namely *H. anaramosae* (Fig. 11E, J, O, T), *H. angusticauda* (Fig. 11D, I, N, S), *H. chini* (Fig. 11A, F, K, P), *H. pseudophthalma* sp. nov. (Fig. 11B, G, L, Q), and *H. sorbei* (Fig. 11C, H, M, R), show small thoracic endopods 3–5 with propodus ending in a dense brush of setae hiding the dactylus with claw. Endopods 6–8 with comparatively slender carpus, propodus, dactylus, and nail; dactylus longer than wide; functional articulation between carpus and propodus. Strong bleaching in Swan medium revealed smaller species-specific differences in thoracic endopod structure (Fig. 11) compared with certain literature data (see Discussion). In the five species examined, the dactylus of thoracic endopods 3–5 bears a single claw opposed by a pair of modified, basally thick paradactylary setae (Fig. 11F–J) from the propodus, resulting in two soft tweezers opposing one solid tweezer. Propodi and dactyli 6–8 separate, not fused with nail (Fig. 11K–O); propodi with a single, stiff seta at conjunction with dactylus; dactyli without seta. Carpi 6–8 are 3-segmented; basal and median segments together contributing less than a quarter of total carpus length. Nails 6–8 smooth, weakly bent, resembling tent pegs due to longitudinal groove at least in basal portions.

Discussion

Validity of *Hansenomysis pseudophthalma* sp. nov.—Not counting the processes on the anterior margin of the carapace, the new species shares the acute or blunt tooth-like processes of the carapace with seven out of 18 so far acknowledged species in this genus:

H. anaramosae San Vicente & Sorbe, 2008 (described above): from 540–2086 m depth in the Bellingshausen Sea and the Weddell Sea. It differs from the new species by the lateral margin of the antennal scale lacking setae between the spines and by the carapace anteriorly produced into a small triangular rostrum.

H. angusticauda O. S. Tattersall, 1961 (described above): from 160–2893 m depth in the Ross Sea, Palmer Archipelago, NE of Elephant Island, off Antarctic Peninsula, and in the Weddell Sea. It differs from the new species by the lateral margin of the antennal scale being without setae between the spines, by the pleomeres 4 and 5 being without the caudal tooth-like protrusions, and by the telson having narrow apex.

H. antarctica Holt & Tattersall, 1906: according to San Vicente (2010) this species has a circum-Antarctic distribution, 53°S–76°S, depth 100–400 m. It differs from the new species by the lateral margin of the antennal scale lacking setae between the spines and by a terminally weakly concave telson with length

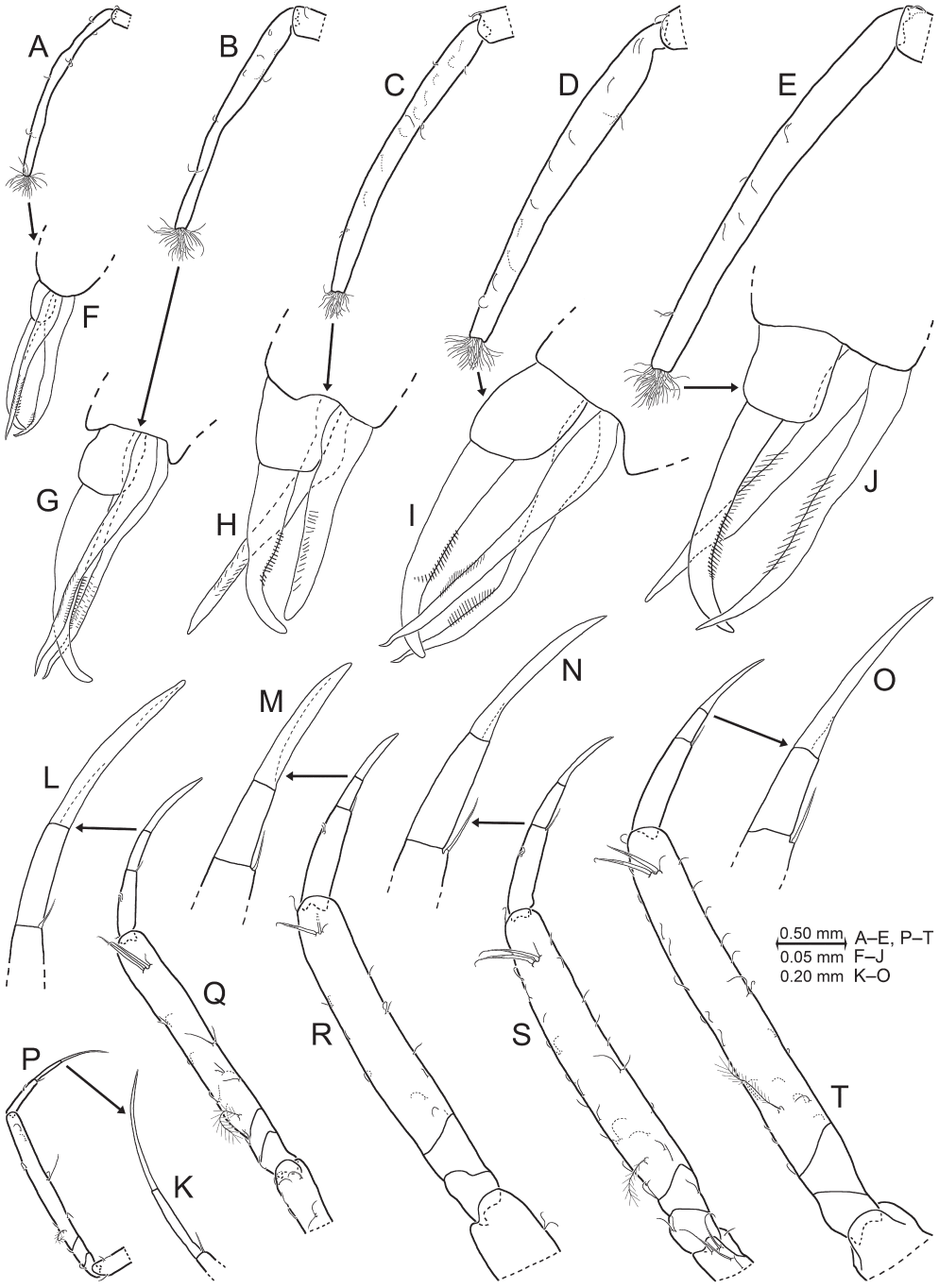

Fig. 11. Tarsus of thoracopods 3, 8 (caudal aspects) in five *Hansenomysis* species: *H. chini* (A, F, K, P; subadult female with BL 11.9 mm), *H. pseudophthalma* sp. nov. (B, G, L, Q; paratype, adult male 22.7 mm), *H. sorbei* (C, H, M, R; adult female 23.9 mm), *H. angusticauda* (D, I, N, S; subadult female 28.2 mm), and *H. anaramosae* (E, J, O, T; adult male 29.7 mm). A–E, tarsus 3, lateral aspect; F–J, dactylus 3 with claw flanked by paradactylary setae, other setae omitted, lateral; K–O, dactylus 8; P–T, tarsus 8.

only three times maximum width.

H. armata Birstein & Tchindonova, 1958: from 2960–3308 m depth in the Kurile-Kamchatka Trench, and in waters off Japan. It differs by a single strong tooth on the midline of the carapace shortly behind the cervical sulcus rather than a cluster of four small teeth (arrow in Fig. 2E) or humps in that position; the mid-caudal carina of the carapace with the rostral edge acute rather than rounded.

H. falklandica O. S. Tattersall, 1955: from 175–1919 m depth in waters off Falkland Islands (Malvinas), Patagonia, Magellan Strait, and off Iceland. It differs from the new species by the more slender antennal scale with the spines up to the tip of the outer margin, by the fewer (about nine) larger spines on the outer margin of the basal segment of the exopod of the uropods. The two carinae posterior to the cervical sulcus of the carapace rise to strong tooth-like projections at about the middle of their length.

H. menziesi Băcescu, 1971: from 1927–1997 m depth in the Peru Trench. It differs by the small triangular rostrum and by the tooth-like lateral projections from the posterior margin of the pleomeres 1–3.

H. sorbei San Vicente, 2009 (described above): from 1579–1869 m depth in Bellingshausen Sea and Powell Basin. It differs by the absence of teeth along the midline of the carapace, and by the presence of tooth-like projections set dorsally and laterally from the posterior margins of the pleomeres 3–6.

Apart from the different structure of the carapace, the five spinous setae on the exopod of male pleopod 2 in *H. pseudophthalma* are in the same size range but more numerous than comparable setae in *H. peruvianus* (two setae in Fig. 5C of Băcescu 1971) and the very similar *H. japonica* (one seta in Fig. 2G, H of Bravo & Murano 1997). In the latter two species these setae extend beyond the tip of exopod 2; not so in *H. pseudophthalma* due to its much longer exopod (15 and 16 segments versus only 6 and 7, respectively).

Identification of *Hansenomysis anaramosae*.—The antennal scale is 4–6 times as long as wide in the present material versus the data given by San Vicente & Sorbe (2008) upon first description of *H. anaramosae*: eight times width in the text (p. 21e6) while 5–6 times for the immature holotype in Fig. 2A, B (op. cit.). As major differences the present adult male with BL 29.7 mm shows longer penes (extending to the ischium of the thoracic endopods) and longer pleopods 1–5 with 1, 16, 18, 13, and 3-segmented endopods, and 18, 18, 18, 18, and 17-segmented exopods, respectively. By contrast, the male paratype with BL 29.0 mm described by San Vicente & Sorbe (2008), shows shorter penes (not extending to the ischium) and the endopods of pleopods 1–5 with only 1, 11, ?, 6, (3?) segments, the exopods with 12, 11, 10, 9, 11 segments, altogether indicative of less advanced sexual maturity. San Vicente & Sorbe (2008) described even shorter penes and less developed pleopods in the immature male holotype with body length 22.5 mm. Due to strong coincidence with the holotype in the complex structure of the eyes, carapace, pleon and telson, the present (well preserved) adult male is identified as belonging to *H. anaramosae* and its sexual characteristics are integrated into the morphological concept of this species.

Structure of thoracic endopods.—Already Hansen (1887) noted [transl.] two "spines" from the "sixth" segment opposing a "spine-like seventh" segment in *Hansenomysis fyllae* (as *Arctomysis Fyllae*), in current interpretation two paradactylary setae from the propodus opposing the dactylus with claw. For *H. antarctica*, O. S. Tattersall (1955) reported thoracic endopods 3–5 ".... terminating, as in other species of the genus, in a minute chela ...." and endopods 6–8 with ".... dactylus long and slender, fused with the long nail to form a long, slender claw". Without discussion of Hansen's finding of a trifid termination of endopods 3–5, she in-

cluded bifid chelae 3–5 together with dactyli 6–8 fused with nail in the definition of the genus *Hansenomysis*. Băcescu (1971) and Bravo & Murano (1997) adopted her interpretation. Băcescu (1971: Figs. 1C, 4B, 8F) drew the bifid chelae for *H. menziesi* and *H. chini*, and drew the dactylus fused with the nail for *H. peruvianus*. Upon description of *H. sorbei*, San Vicente (2009) stressed that endopods 3–5 are "forming minute chelate structure" and that "dactylus and nail together" form "a long claw-like termination" of endopods 6–8. No modified setae are given in his drawings (Fig. 3C, E) of the distal part of propodi 4, 5. Birstein & Tchindonova (1958) were the first to again pick up on Hansen's (1887) interpretation of the three claw-like elements at the tip of the endopods 3–5, namely the dactylus with the claw opposed by the two thickened setae from the propodus in *H. armata*. In line with this, Lagardére (1983) interpreted the three elements as forming a "pince tridactyle" in *H. nouveli* and *H. pseudofyllae*. For these species he reported that the dactyli 6–8 were prolonged by a long and fine nail not fused with the dactylus, together visualized by him in Fig. 72 for *H. atlantica* Lagardére, 1983, this taxon currently acknowledged as *Bacescomysis atlantica* (Lagardére, 1983). The here examined thoracic endopods (Fig. 11) of *H. anaramosae*, *H. angusticauda*, *H. chini*, *H. pseudophthalma*, and *H. sorbei* fit with the findings and interpretation by Lagardére (1983). The textual description of *H. angusticauda* by O. S. Tattersall (1961: p. 563) and the respective drawings for *H. chini* and *H. sorbei* by Băcescu (1971) and San Vicente (2009) are revised in present Fig. 11 accordingly. The dense brush of setae at the apex together with vicinity to the mouth field suggest that thoracic endopods 3–5 are capable of brushing food from the substrate surface and of transferring food to the mouth area. The dactyli 3–5 including their claw and paradactylary setae are completely embedded in the apical setae brush (Fig. 11A–E). This suggests that the minute, apical, triplicate tweezers (Fig. 11F–J) of endopods 3–5 could be capable of picking up and transferring 'immotile' food rather than having a more predatory function. The long, slender endopods 6 and 7, in part also 8 (Figs. 7L, 11N–P), with slender nails (Fig. 7K) appear suitable for clinging rather than walking. The nails 6–8 of the five species examined, most distinctly in nails 8 of *H. sorbei* and *H. pseudophthalma*, are laterally slightly flattened with a longitudinal groove (best visible in Fig. 7K, L), resembling tent-pegs and possibly useful for holding onto soft substrate.

Eye structure and development.—Inspection in dorsal and lateral view revealed small distally projecting lateral processes of the eye rudiments in all five *Hansenomysis* here examined. The lateral processes were previously unknown or misinterpreted in all three species with (additional) paramedian processes. The lateral processes have previously not been reported for *H. anaramosae* and *H. sorbei*. O. S. Tattersall (1961: Fig. 6) drew the lateral processes as emerging from the frons, but not from the eye rudiment for *H. angusticauda*, and did not comment this in the text. Numbers of eye processes are important for taxonomy at species level, exemplified also by species-specific numbers in the present material. Accordingly, the revised numbers are integrated into the above diagnoses but not included in the above key due to missing data on other species.

Already Lagardère (1983) noted that the 'horns' of the 'eyeplate' are feebly developed in juveniles of *H. pseudofyllae* but prominent in adult females. For a subadult male he drew bulbous (? inside) structures of the 'eyeplate', but not so for an adult female (Fig. 19 versus Fig. 21 *op. cit.*), and did not comment this in the text. Comparable observations (Fig. 10) were made in all *Hansenomysis* species for which sufficient material was available in the here examined ANDEEP collections: *H. anaramosae*, *H. pseudophthalma*, and *H. sorbei*. The juveniles show separate eye bulbs within a

fused sheath (Fig. 10A). Measured without distal projections, the dorsoventral extension of the sheath surpasses the longitudinal extension. The sheath is thus bar-like rather than plate-like as suggested by the commonly used term 'eyeplate'. Relative antero-posterior extension of the bars decreases and the length of paired anterior processes, if any, increases in the course of individual growth. These growth changes appear important for diagnoses and distinction of taxa, particularly if only non-adults are available.

Structure and biological function of photophores.—As shown above, adults of *H. pseudophthalma* sp. nov. (Figs. 3A–C, E, 4B) and *H. chini* (Fig. 1A, B) bear calotte-shaped bulges resembling eyes in the hepatic area on either side of the carapace. The distal hyaline area of modified bulges could represent lenses in *H. pseudophthalma* (Fig. 3B) and *H. sorbei* (Fig. 9D). Overall, the detailed structures in Fig. 3B, E are concluded as being indicative of photophores distally on the hepatic bulges in *H. pseudophthalma*. The photophores strongly resemble the epidermal luminescent organs described by Terao (1917) in thoracic sternites of the decapod *Lucensosergia lucens* (Hansen, 1922), reported by him as *Sergestes prehensilis*. The distally directed, parallel lamellar structures (interpreted as photocytes; Fig. 3E) in the distal cushion of hepatic bulges in *H. pseudophthalma* also show some resemblance with those figured by Bracken-Grissom *et al.* (2020: Fig. 1A) for pleopod photophores of the deep-sea decapod *Janicella spinicauda* (A. Milne-Edwards, 1883). Tattersall & Tattersall (1951) argued that the lophogastrid "*Gnathophausia* is the only Mysidacean in which a luminous organ has been described, though other forms have been vaguely referred to as phosphorescent". In line with this, Herring & Gruner (2004) concluded that early reports of luminescence in the Mysidae Haworth, 1825, genera *Siriella* Dana, 1850, and *Gastrosaccus* Norman, 1868, have not been verified. This suggests that the present records in Petalophthalmidae provide first verifiable evidence of photophores also in the superior taxonomic category, namely in the order Mysida. Cartes (2009) argued that bioluminescence was involved in "prey attraction, warding off predators, formation of shoals, reproductive behavior, etc." According to Herring & Gruner (2004) the integumental photophores of euphausiaceans and decapods emit their light in ventral direction. They conclude this, together with the reduction or absence of the ventral photophores in bathypelagic species, as being indicative of counter-illumination camouflage in epi- to mesopelagic species. Such a function appears unlikely in *H. pseudophthalma* because the photophores face obliquely anteriorly and are also based on the so far known exclusively bathybenthic distribution of this species. According to Herring & Gruner (2004) there is no evidence that crustaceans emit light to locate food or attract prey. Predatory behavior is excluded in *H. pseudophthalma* due to thin thoracic appendages with weak claws in combination with normal-sized mouthparts. The exclusive occurrence of mature photophores in adults points to a possible role in reproductive behavior. There are, however, no visual elements in the reduced eyes of *Hansenomysis* species. Extraocular photoreception cannot be excluded because this is precisely what Bracken-Grissom *et al.* (2020) reported in the photophores of certain decapods. Accordingly, the eyelike appearance (Figs. 1A, B, 3A) of *Hansenomysis* photophores could be related to photoreception. Research on living specimens would be most welcome to answer such questions and shed further light on bioluminescence in this genus.

Acknowledgements

The author is greatly indebted to Angelika Brandt (Frankfurt) and Ute Mühlenhardt-Siegel (Hamburg) for helpful advice on examination of ANDEEP mysids. Sincere thanks to Nancy

Mercado Salas, Kathrin Philipps-Bussau and Petra Wagner from the Zoological Museum Hamburg for their efforts and patience with longstanding loans of materials.

■ Literature Cited

Astthorsson, O. S., & Brattegard, T., 2022. Distribution and biology of Lophogastrida and Mysida (Crustacea) in Icelandic waters. Fjölrit Náttúrufræðistofnunar, 58: 1–114.

Băcescu, M., 1967. Further mysids from the Pacific Ocean collected during the XIth cruise of R/V Anton Bruun, 1965. Revue Roumaine de Biologie–Zoologie, 12: 147–159.

Băcescu, M., 1971. Contributions to the Mysid Crustacea from the Peru-Chile Trench (Pacific Ocean). In: Scientific Results of the Southeast Pacific Expedition. Anton Bruun Report, 7: 3–24.

Bellamy, C. L., 2006. Insecta Coleoptera Buprestidae of Madagascar and Adjacent Islands. An Annotated Catalogue. Faune de Madagascar, 92: 5–267. IRD Editions, Paris et Montpellier.

Birstein, J. A., & Tchindonova, Yu. G., 1958. Glibocovodnie misidii severo-zapadnoi tschasii Tihogo Okeana [The deep sea mysids of the northwest Pacific Ocean]. Trudy Instituta Okeanologii Akademii Nauk SSSR, 27: 258–355.

Birstein, J. A., & Tchindonova, Yu. G., 1970. New mysids (Crustacea, Mysidacea) from the Kurile-Kamtchatka Trench. Trudy Instituta Okeanologii Akademii Nauk SSSR, 86: 277–291.

Boas, J. E. V., 1883. Studien über die Verwandtschaftsbeziehungen der Malakostraken. Morphologisches Jahrbuch, 8: 485–579, pls. XXI–XXIV. Wilhelm Engelmann, Leipzig.

Bracken-Grissom, H. D., DeLeo, D. M., Porter, M. L., Iwanicki, T., Sickles, J., & Frank, T. M., 2020. Light organ photosensitivity in deep-sea shrimp may suggest a novel role in counterillumination. Scientific Reports, 10: 4485.

Brandt, A., Brenke, N., Mühlenhardt-Siegel, U., & Wägele, J. W, 2006. 1. 4. 6 Macrofauna represented in sledge-samples. In: W. Balzer, J. Alheit, K. C. Emeis, H. U. Lass, & M. Türkay, (eds.), South-East Atlantic 2000, Leg M48/1; Cruise No. 48, 6 July 2000–3 November 2000, Walvis Bay–Walvis Bay. Meteor-Berichte, 06–5: 1–22 to 1–26.

Brandt, A., Brix, S., Brökeland, W., Choudhury, M., Kaiser, S., & Malyutina, M., 2007. Deep-sea isopod biodiversity, abundance, and endemism in the Atlantic sector of the Southern Ocean—Results from the ANDEEP I–III expeditions. Deep-Sea Research Part II: Topical Studies in Oceanography, 54: 1760–1775.

Brandt, A., De Broyer, C., Gooday, A. J., Hilbig, B., & Thomson, M. R. A, 2003. Introduction to ANDEEP (ANtarctic benthic DEEP-sea biodiversity: colonization history and recent community patterns)—a tribute to Howard L. Sanders. Deep-Sea Research Part II: Topical Studies in Oceanography, 470: 45–49.

Brandt, A., Mühlenhardt-Siegel, U., & Siegel, V., 1998. An account of the Mysidacea (Crustacea, Malacostraca) of the Southern Ocean. Antarctic Science, 10: 3–11.

Bravo, M. R., & Murano, M., 1997. New records of the genus *Hansenomysis* in Japan with description of a new species (Crustacea: Mysidacea: Petalophthalmidae). Proceedings of the Biological Society of Washington, 110: 227–235.

Cartes, J. E., 2009. Adaptations to Life in the Oceans. Pelagic Macrofauna. In: C. M. Duarte, & A. Lota, (eds.), Encyclopedia of Life Support Systems (EOLSS). Marine Ecology, 1: 168–198.

Casanova, J.-P., 1993. Crustacea Mysidacea: Les Mysidacés Lophogastrida et Mysida (Petalophthalmidae) de la région neo-calédonienne. In: A. Crosnier, (ed.), Résultats des Campagnes MUSORSTOM, Vol. 10 (3). Mémoires du Muséum national d'Histoire naturelle, série A, Zoologie, 156: 33–53.

Czerniavsky, V., 1882. Monographia Mysidarum inprimis Imperii Rossici (marin., lacustr. et fluviatilium). Fasc. 1. Trudy Sankt-Peterburgskago obshchestva estestvoispytatelei, 12(2): 1–170.

Czerniavsky, V., 1887. Monographia Mysidarum inprimis Imperii Rossici (marin., lacustr. et fluviatilium). Fasc. 3. Trudy Sankt-Peterburgskago obshchestva estestvoispytatelei, 18: i–viii, 1–102, pls. V–XXXII.

Dana, J. D., 1850. Synopsis generum Crustaceorum ordinis "Schizopoda". American Journal of Science and Arts, ser. 2, 9(25): 129–133.

Fahrbach, E., (ed.), 2006. The expedition ANTARKTIS-XXII/3 of the research vessel "Polarstern" in 2005. Berichte zur Polar- und Meeresforschung, 533: 1–246.

Faxon, W., 1893. Reports on the dredging operations off the west coast of Central America to the Galápagos, to the west coast of Mexico, and the Gulf of California; in charge of Alexander Agassiz, carried on by the U.S. Fish Commission Steamer Albatross during 1891. VI. Preliminary descriptions of new species of Crustacea. Bulletin of the Museum of Comparative Zoölogy at Harvard College, 24(7): 149–220.

Fukuoka, K., 2009. Deep-sea mysidaceans (Crustacea: Lophogastrida and Mysida) from the northwestern North Pacific off Japan, with descriptions of six new species. In: T. Fujita, (ed.), Deep-sea fauna and pollutants off Pacific coast of northern Japan. National Museum of Nature and Science Monographs, 39: 405–446.

Fütterer, D. K., Brandt, A., & Poore, G. C. B., (eds.), 2003. The Expeditions ANTARKTIS-XIX/3–4 of the Research Vessel POLARSTERN in 2002 (ANDEEP I and II: Antarctic benthic deep-sea biodiversity-colonization history and recent community patterns). Berichte zur Polar- und Meeresforschung, 470: 1–174.

Hansen, H. J., 1887. Malacostraca marina Groenlandiae occidentalis. Oversigt over det vestlige Grønlands fauna af malakostrake Havkrebsdyr. Videnskabelige Meddelelser fra den Naturhistoriske Forening i Kjobenhavn, ser. 4, 9: 5–226, Tav. II–VII, 1 map.

Hansen, H. J., 1922. Crustacés Décapodes (Sergestides) provenant des campagnes des yachts Hirondelle et Princesse-Alice (1885–1915). In: M. J. Richard, (ed.), Résultats des campagnes scientifiques accomplies sur son yacht par Albert Ier, fasc. 64: 3–232, pls. I–XI. Imprimerie de Monaco.

Haworth, A. H., 1825. XXIX. A new binary arrangement of the Macrurous Crustacea. The Philosophical Magazine and Journal, London, 65(323): 183–184.

Herring, P. J., & Gruner, H.-E., 2004. Luminous organs and luminescence. In: J. Forest, & J. C. von Vaupel Klein, (eds.), The Crustacea. Revised and updated from the Traité de Zoologie, 1(8): 381–413. Brill, Leiden.

Holt, E. W. L., & Tattersall, W. M., 1906. Preliminary notice of the Schizopoda collected by H.M.S. Discovery in the Antarctic region. Annals and Magazine of natural History, ser. 7, 17: 1–11.

Howe, J. A., 2003. Chapter 3.4.2. Recent depositional environments of the north western Weddell Sandwich Trench. In: D. K. Fütterer, A. Brandt, & G. C. B. Poore, (eds.), The Expeditions ANTARKTIS-XIX/3–4 of the Research Vessel POLARSTERN in 2002 (ANDEEP I and II: Antarctic benthic deep-sea biodiversity-colonization history and recent community patterns). Berichte zur Polar- und Meeresforschung, 470: 124–126.

Howe, J. A., 2006. Chapter 9.4.2. Recent sedimentation and geochemistry across the Northern Weddell Sea and adjacent deep-water regions, Antarctica. In: E. Fahrbach, (ed.), The expedition ANTARKTIS-XXII/3 of the research vessel "Polarstern" in 2005. Berichte zur Polar- und Meeresforschung, 533: 196–208.

Lagardère, J.-P., 1983. Les mysidacés de la plaine abyssale du Golfe de Gascogne 1. Familles des Lophogastridae, Eucopiidae et Petalophthalmidae. Bulletin du Muséum national

d'Histoire naturelle, 4ème série, section A (Zoologie, Biologie, Écologie animale), 5(3): 809–843.

Ledoyer, M., 1977. *Ceratomysis ericula* n.sp. (Crustacea, Mysidacea) recoltée au large des Iles Kerguelen. Bulletin du Muséum national d'Histoire naturelle, 3ème série, section Zoologie, 432: 253–258.

Mauchline, J., & Murano, M., 1977. World list of the Mysidacea, Crustacea. Journal of the Tokyo University of Fisheries, 64: 39–88.

Mees, J., & Meland, K., (eds.), 2022. World List of Lophogastrida, Stygiomysida and Mysida. *Hansenomysis* Stebbing, 1893. Accessed through: World Register of Marine Species (URL: https://www.marinespecies.org/aphia.php?p=taxdetails&id=119913).

Milne-Edwards, A., 1883. Recueil de figures de Crustacés nouveaux ou peux connus. In: J. Forest, & L. B. Holthuis, (eds.), facsimile edition, 1997: 1–128. Backhyus Publishers, Leiden.

Norman, A. M., 1868. Preliminary report on the Crustacea, Molluscoida, Echinodermata, and Coelenterata, procured by the Shetland Dredging Committee in 1867. Reports of the British Association for the Advancement of Science, 37(1867): 437–441.

Petryashov, V. V., 2005. Mysids (Crustacea, Mysidacea) collected by Soviet and Russian Antarctic expeditions. Lophogastrida, Petalophthalmida, and Mysida: Boreomysidae. Zoologicheskij Zhurnal, 84(8): 957–973.

Petryashov, V. V., 2014. Chapter 5.16. Lophogastrida and Mysida (Crustacea: Malacostraca: Peracarida) of the Southern Ocean. In: C. De Broyer, P. Koubbi, H. J. Griffiths, B. Raymond, C. d'Udekem d'Acoz, *et al.*, (eds.), Biogeographic Atlas of the Southern Ocean (CoML/CAML Atlas). Census of Antarctic Marine Life. SCAR-Marine Biodiversity Information Network, 149–154. Scientific Commitee on Antarctic Research, Cambridge.

Price, W. W., 2001. World list of Mysidacea. NeMys doc_id 3677. (URL: http://www.marinespecies.org/aphia.php?p=sourcedetails&id=4191)

Price, W. W., 2004. An annotated checklist for the order Mysida (Crustacea: Malacostraca: Peracarida) from the Pacific coasts of the Americas (Alaska to Chile). In: M. E. Hendrickx, (ed.), Contributions to the study of East Pacific crustaceans, 3: 53–77. Instituto de Ciencias del Mar y Limnologia, UNAM.

San Vicente, C., 2009. *Hansenomysis sorbei* sp. nov., a new suprabenthic mysid (Crustacea: Mysida: Petalophthalmidae) from the Bellingshausen Sea (Southern Ocean). Zootaxa, 2240: 31–40.

San Vicente, C., 2010. Species Diversity of Antarctic Mysids (Crustacea: Lophogastrida and Mysida). In: T. J. Mulder, (ed.), Antarctica: Global, Environmental and Economic Issues, Chapter 1: 1–80. Nova Science Publishers.

San Vicente, C., & Sorbe, J.-C., 2008. *Hansenomysis anaramosae* sp. nov., a new suprabenthic mysid (Crustacea: Mysidacea: Petalophthalmidae) from the Bellingshausen Sea (Southern Ocean). Organisms, Diversity & Evolution, 8: 21.e1–21.e9.

Spinola, M., 1837. Lettre adressée à la Société entomologique de France sur un groupe de Buprestides. Annales de la Société entomologique de France, 6: 101–122 [not seen].

Stebbing, T. R. R., 1893. A history of the Crustacea. Recent Malacostraca. The International Scientific Series, (American ed.), 71: i–xvii, 1–466, pls. I–XIX. D. Appleton & Co., New York.

Tattersall, O. S., 1955. Mysidacea. Discovery Reports, 28: 1–190. Cambridge University Press.

Tattersall, O. S., 1961. Report on some Mysidacea from the deeper waters of the Ross Sea. Proceedings of the Zoological Society of London, 137: 553–571.

Tattersall, W. M., & Tattersall, O. S., 1951. The British Mysidacea. Ray Society Monograph 136: 1–460. The Ray Society, London.

Terao, A., 1917. Notes on the Photophores of *Sergestes prehensilis* Bate. Annotationes Zoologicae Japonensis, 9: 299–316.

Thomson, J., 1878. Buprestides Polybothroides. Revue et Magasin de Zoologie, 3 (6): 313–349.

Wittmann, K. J., 2013. Comparative morphology of the external male genitalia in Lophogastrida, Stygiomysida, and Mysida (Crustacea, Eumalacostraca). Zoomorphology, 132: 389–401.

Wittmann, K. J., 2020. Lophogastrida and Mysida (Crustacea) of the "DIVA-1" deep-sea expedition to the Angola Basin (SE-Atlantic). European Journal of Taxonomy, 628: 1–43.

Wittmann, K. J., Ariani, A. P., & Lagardère, J.-P., 2014. Orders Lophogastrida Boas, 1883, Stygiomysida Tchindonova, 1981, and Mysida Boas, 1883 (also known collectively as Mysidacea). In: J. C. von Vaupel Klein, M. Charmantier-Daures, & F. R. Schram, (eds.), Treatise on Zoology-Anatomy, Taxonomy, Biology. The Crustacea. Revised and updated, as well as extended from the Traité de Zoologie, 4 Part B (54): 189–396; color pls. 404–406. Brill, Leiden.

Wittmann, K. J., & Chevaldonné, P., 2021. First report of the order Mysida (Crustacea) in Antarctic marine ice caves, with description of a new species of *Pseudomma* and investigations on the taxonomy, morphology and life habits of *Mysidetes* species. ZooKeys, 1079: 145–227, suppl. 1.

Address
Medical University of Vienna, Department of Environmental Health, Kinderspitalgasse 15, A-1090 Vienna, Austria

E-mail
karl.wittmann@meduniwien.ac.at